Biocolorants for engineering materials

Juha Jordan

Aalto University

Aalto University publication series
Doctoral Theses 198/2025

Biocolorants for engineering materials

Juha Jordan

A doctoral thesis completed for the degree of Doctor of Science to be defended, with the permission of the Aalto University School of Chemical Engineering at a public examination held at the lecture hall KE2 of the school on 17th October 2025 at 12:00.

Aalto University
School of Chemical Engineering
Department of Chemistry and Materials Science

Supervising professor
Professor Jaana Vapaavuori, Aalto University, Finland

Thesis advisor
Doctor Päivi Laaksonen, Häme University of Applied Sciences, Finland

Preliminary examiners
Professor Dorien Derksen, AVANS University of Applied Sciences, Netherlands
Docent Sami Hietala, University of Helsinki, Finland

Opponent
Assistant Professor Tero-Petri Ruoko, Tampere University, Finland

Aalto University publication series
Doctoral Theses 198/2025

Image on the cover by Juha Jordan

ISBN 978-952-64-2767-6 (soft cover)
ISBN 978-952-64-2766-9 (PDF)
ISSN 1799-4934 (printed)
ISSN 1799-4942 (PDF)

http://urn.fi/URN:ISBN:978-952-64-2766-9

Unigrafia Oy
Helsinki 2025

ABSTRACT

Author Juha Jordan

Name of the doctoral thesis Biocolorants for engineering materials

Article-based thesis

Number of pages 105

Keywords Biocolorants, engineering materials, long-term durability

Even though colorants are rarely thought of as independent materials, colors of most human-made objects are artificially altered by applying colorant additives. Biocolorants, which are colorants from bio-based sources, offer sustainable alternatives to the currently prevalent synthetic colorants originating from petrochemical sources. However, perhaps due to the long history of using biocolorants in textile coloration, modern research has primarily focused on utilizing biocolorants in textile field. Consequently, research of biocolorants in engineering materials has received much less attention.

The objective of this thesis was to find practical and durable solutions for using biocolorants in engineering materials. Thus, bio-based indigo from *Isatis tinctoria* was utilized in coloration of wood coatings, polypropylene, and polylactic acid. In addition to indigo, madder (*Rubia tinctorum*) extract, weld (*Reseda luteola*) extract, kraft lignin, and biochar were used for biocoloration of polylactic acid. Furthermore, dyeing of anodized aluminum surface was explored utilizing madder and weld extracts as biocolorants. Besides initial color properties, durability performance of the biocolored materials was determined by exposure to either cyclical artificial weathering or continuous Xenon light, followed by colorimetric and spectral re-evaluation.

The results showed that weathering resistance of the wood coatings colored with bio-based indigo pigment was comparable to the coatings utilizing a commercial mineral pigment. Moreover, purification of the bio-based indigo pigment improved its color strength and lightfastness even further when used for polypropylene coloration. Nevertheless, even more promising biocoloration results for polylactic acid were achieved using kraft lignin pigment, which produced a stable color and improved both photodegradation resistance and mechanical performance of the polylactic acid matrix. Finally, biocoloration of anodized aluminum with madder and weld extracts successfully produced thin colored layers with even and intense metallic colors.

In summary, this thesis showcases promising real-world applications for biocolorant use in coloration of engineering materials, while focusing specifically on durability and applicability performances of the studied biocolorants.

TIIVISTELMÄ

Tekijä Juha Jordan

Väitöskirjan nimi Teknisten materiaalien värjääminen bioväriaineilla

Artikkeliväitöskirja

Sivumäärä 105

Avainsanat Bioväriaineet, tekniset materiaalit, pitkäaikaiskestävyys

Vaikka väriaineita käsitellään irrallaan muista materiaaleista vain harvoin, suurin osa ihmiskunnan tuotoksista on keinotekoisesti värjätty väriaineita käyttäen. Biopohjaisista raaka-aineista tuotetut väriaineet eli bioväriaineet tarjoavat puhtaamman vaihtoehdon nykyään laajalti käytettäville synteettisille väriaineille, jotka tuotetaan fossiilisista polttoaineista jalostamalla. Moderni bioväriainetutkimus on kuitenkin keskittynyt suurelta osin tekstiilien biovärjäyksen tutkimiseen, sillä bioväriaineita on käytetty laajalti kankaiden värjäämisessä jo kauan ennen synteettisten väriaineiden keksimistä. Tämän seurauksena teknisten materiaalien värjäämistä bioväriaineilla on tutkittu huomattavasti vähemmän.

Tämän väitöskirjan tavoitteena oli löytää käytännöllisiä ja pitkäaikaiskestäviä bioväriaineita teknisten materiaalien värjäämiseen. Ensimmäiset tutkimukset keskittyivät puupinnoitteiden, polypropeenin, sekä polylaktidin biovärjäämiseen värimorsingosta (*Isatis tinctoria*) peräisin olevalla indigopigmentillä. Polylaktidin värjäämistä tutkittiin indigon lisäksi myös värimatarasta (*Rubia tinctorum*) ja väriresedasta (*Reseda luteola*) uutetuilla väriaineilla sekä kraftligniinillä ja biohiilellä. Lisäksi tutkittiin myös anodisoidun alumiinipinnan värjäämistä sekä matara- että resedauuttella. Tavanomaisten väriominaisuuksien lisäksi värjättyjen materiaalien pitkäaikaiskestävyyttä arvioitiin altistamalla materiaaleja joko keinotekoiselle säärasitukselle tai jatkuvalle Xenon-valolle, minkä jälkeen altistettujen materiaalien väri- ja spektriominaisuuksia arvioitiin uudelleen.

Tulokset osoittivat, että puupinnoitteissa biopohjaisella indigopigmentillä saavutettiin kaupalliseen mineraalipigmenttiin verrattavissa oleva säänkesto. Lisäksi biopohjaisen indigopigmentin värin voimakkuutta ja valonkestoa polypropeenimuovissa kyettiin parantamaan edelleen pigmentin happopuhdistuksella. Polylaktidin värjäämisessä lupaavimmat tulokset saavutettiin kraftligniinillä, joka paransi valonkeston lisäksi myös polylaktidin lujuusominaisuuksia. Myös anodisoidun alumiinin värjääminen onnistui ja tuotti tulokseksi ohuen, voimakkaan metallivärisen oksidipinnoitteen.

Yhteenvetona, tässä väitöskirjassa esitellään lupaavia ratkaisuja bioväriaineiden käyttöön teknisten materiaalien värjäämisessä, keskittyen eritoten värjättyjen materiaalien pitkäaikaiskestävyyteen ja käytettävyyteen reaalimaailman olosuhteissa.

Acknowledgements

Finally, I’m writing the part I’ve been thinking about since I started working on my thesis. Like many others before me, I ended my master’s studies convinced that academia was not quite for me. Yet, when this opportunity was offered to me, I welcomed it with little hesitation. Why? During the six years of working on this thesis, I used to praise my curiosity on good days and blame my impulsiveness on bad days. Whatever the case, it no longer matters – the work is finished, and it brings me both happiness and a sense of confusion at the same time.

Almost all work for this thesis was carried out at Häme University of Applied Sciences in the Long-Term Durability research group. Some experiments were also conducted in Technological University of the Shannon: Midlands during my two-week visit to Athlone, Ireland. Furthermore, funding for this thesis was mostly provided by the Academy of Finland project BioColour. In addition, part of my research work was also financially supported by UNELMAT project, which was funded by Hauho and Renko Bank Foundations. I am very grateful for both funders, as their contribution allowed me to concentrate on my work without needing to worry about money too much.

Now that you know how I ended up here and who paid the costs, it is time to give my sincerest thanks to the people who helped along the way. First and most importantly, special thanks to my research group leader and thesis advisor Dr. Päivi Laaksonen for all the support, guidance and organizing you have done over the years. It is still a mystery to me how you always seemed to believe in my graduation at the times I felt completely stuck. Same goes to Prof. Jaana Vapaavuori, my supervisor in Aalto, your positivity has motivated me so much! Also, thanks to Asst. Prof. Tero-Petri Ruoko for being my opponent and to Prof. Dorien Derksen and Doc. Sami Hietala for pre-examining my work. Finally, Sirje, thank you for your timely reminders to progress the practical aspects of the thesis work! Without you, my estimated year of graduation would have probably been around 2030…

Big thanks to my co-workers at HAMK as well, especially Johanna, Kalle, Nea, Päivi L-P, Riikka, Roosa, Tiina, and Ville. You have successfully prevented me from losing myself to the writing void countless times. Tielidy, thank you for taking care of me in Athlone and introducing me to the local academics! As odd as it might

sound, thanks to you, I experienced more connections to other Ph.D. students during my two-week visit in Ireland than during my six years of working in Finland.

In addition to my colleagues, I would like to wholeheartedly thank the numerous people in my private life, who enrich my earthly journey with meaning and laughter. First, huge thanks to my friends from the magical underground hobbies, Fose, Joni, Pahvi, Saku, and everyone else too! You were the first people to show me how to let go and have fun – a life lesson that is heavily undervalued in this performance-oriented world. Nothing replenishes sanity better than getting lured to totally random adventures. Well, except maybe throwing frisbees in the woods, so deserved thanks to my more recent friends for keeping me company there! Our rounds have always succeeded in returning my brain to the PhD fairway even when I have felt quite out of bounds beforehand.

Moving on from pure friendships to family matters, I have to express the biggest thanks to my wife, life partner, best friend, and co-brain Iiris. No one supports me like you do, no one knows me like you do, and no one believes in me like you do. You are simply invaluable to me, and I am glad that we have chosen to spend our time on earth together. Moreover, huge thanks to my parents, brothers, grandparents, and my uncle for providing me with the happiest and safest childhood. The best part is that you're all still incredibly fun to spend time with even now that we are all adults – a feat that should by no means be taken for granted!

Hämeenlinna, 16th September 2025
Juha Jordan

Contents

List of Abbreviations and Symbols

ATR	Attenuated total reflection
BV	Boat varnish
CI	Carbonyl index
CR	Contrast ratio
DMSO	Dimethyl sulfoxide
EP	Exterior primer paint
FTIR	Fourier-transform infrared (spectroscopy)
HSI	Hyperspectral imaging
LOP	Linseed oil paint
PLA	Polylactic acid
PP	Polypropylene
RH	Relative humidity
rpm	Rotations per minute
SEM	Scanning electron microscopy
TGA	Thermogravimetric analysis
UT	Universal thinner
UV-vis	Ultraviolet-visual (spectroscopy)

List of Publications

This doctoral dissertation consists of a summary and of the following publications which are referred to in the text by their numerals

I. Jordan, Juha; Helander, Roosa; Laaksonen, Päivi. 2021. Colour stability of wood coatings pigmented with natural indigo from Isatis tinctoria after accelerated weathering. Wiley-Blackwell. *Coloration Technology*, volume 138, issue 2, pages 210-218. ISSN 1472-3581. https://doi.org/10.1111/cote.12585

II. Jordan, Juha; de Morais de Lima, Tielidy Angelina; Nugent, Michael; Laaksonen, Päivi. 2025. Lightfastness of polypropylene pigmented with natural indigo of Isatis Tinctoria. Emerald Publishing Group. *Pigment & Resin Technology*. https://doi.org/10.1108/PRT-03-2024-0026

III. Jordan, Juha; de Morais de Lima, Tielidy Angelina; Nugent, Michael; Laaksonen, Päivi. 2024. Effect of organic biocolourants on lightfastness and mechanical properties of polylactic acid. Wiley-Blackwell. *Coloration Technology*. Advance online publication. https://doi.org/10.1111/cote.12803

Author's Contribution

Publication I: Colour stability of wood coatings pigmented with natural indigo from *Isatis tinctoria* after accelerated weathering

JJ and PL conceptualized the experiments. JJ prepared the pigment powders and designed and prepared the coating formulations. JJ and RH coated wooden panels and carried out the artificial weathering experiments. JJ performed all the other experiments alone. JJ analyzed the results and prepared the initial manuscript, which was reviewed and edited by all authors.

Publication II: Lightfastness of polypropylene pigmented with natural indigo of *Isatis Tinctoria*

JJ and PL conceptualized the experiments and designed the pigment purification process. JJ prepared the pigment powders and carried out the pigment purification. TL did TGA measurements for the pigments and collaborated with JJ in the ATR-FTIR measurements. JJ designed and prepared the pigment solutions and pigmented specimen rods. JJ performed all experiments and analyses related to the pigment solutions and pigmented specimen rods alone. JJ fully analyzed the results from all experiments and prepared the initial manuscript, which was reviewed and edited by all authors.

Publication III: Effect of organic biocolourants on lightfastness and mechanical properties of polylactic acid

JJ and PL conceptualized the experiments. JJ prepared and analyzed the biocolorant powders and designed the biocolored specimens. JJ and TL prepared the specimens and carried out the mechanical testing together. JJ did the other experiments and fully analyzed the results from all the experiments alone. JJ prepared the initial manuscript, which was reviewed and edited by all authors.

1. Introduction

1.1 Colorants, biocolorants, and sustainability of color

Colorants, the substances that can be used to color materials, are present everywhere in the modern urban environment.[1] They are hidden in plain sight, for instance, in dyed fabrics, coated surfaces, pigmented plastics, ink-printed paper, and painted art.[1] Even though colorants are often merely viewed as a source of aesthetic pleasure, they are also vital for human communication and mental health.[2–5] If all colorants suddenly disappeared from human-made materials, any urban environment would become obscure and unfamiliar.[6] The cities would turn into giant mazes dominated by cold shades of metal and concrete accompanied by white or translucent plastics.[7] There would be no books, printed signs, or painted surfaces; all our clothes would be white, brownish, or perhaps even transparent. The colorant-free urban environment would not only be miserable, but almost inhabitable as well.

To create a functioning and healthy urban environment, over 2 million tons of colorants was produced worldwide in 2023, creating an enormous market revenue of 42.6 billion US dollars.[8, 9] Most of the produced colorants were inorganic solid pigments acquired by mining, but approximately 44 % of them were organic water-soluble dyes synthesized from petroleum base.[8] In the 21st century, however, the continuously growing production of synthetic colorants has started to receive criticism due to utilizing non-renewable raw materials and various environmentally hazardous chemicals.[10–12] Moreover, many synthetic colorants are toxic for aquatic organisms, which is a serious issue especially in large-scale textile dyeing processes, where the waste effluent often contains a substantial amount of water-soluble textile dyes.[13–17] Thus, heavy research effort has been put to developing more sustainable and environmentally friendly alternatives to the synthetic colorants. [15, 18]

Biocolorants, which are organic colorants derived from bio-based sources, such as plants, fungi, microbes, or even organic waste, are undoubtedly the most researched alternatives to synthetic colorants.[19–23] Even though biocolorant research has become increasingly popular in the last decades, using biocolorants is not a novel concept, but an ancient practice that has been done for thousands of years.[24–26] As synthetic colorants did not exist in the pre-industrial world, the only options for coloration were either organic biocolorants or mineral pigments.[26, 27] Thus, various dye plant species, such as woad (*Isatis tinctoria*) and weld (*Reseda luteola*), which produce colorants as secondary metabolites, were frequently cultivated in large scale.[25, 28, 29] However, the dye plant cultivation stopped almost completely in the 19th century due to discovery of colorant synthesis and rapid development of new petroleum-based colorants.[30] Even though synthetic colorants still present superior stability and more versatile color palette compared to biocolorants, the modern research efforts have found numerous practical, sustainable, and economically viable applications for biocolorants.[20, 31–36] As a consequence, biocolorants are steadily making a comeback to provide more environmentally friendly options for coloration.

1.2 Objectives of the thesis

The main objective of this thesis was to investigate the viability of biocolorants for coloration of various solid engineering materials. The ultimate goal was to achieve biocolored materials, which could be produced on an industrial scale and used in practical applications. In such materials, the biocolorant should either provide improved sustainability or protective properties compared to equivalent synthetic colorant without causing a negative impact on material durability, color fastness, or accessibility of the material. Thus, special emphasis was placed on studying color fastness and long-term durability properties of the biocolored materials. Furthermore, availability and fastness properties were used as initial selection criteria for the biocolorants used in this thesis.

1.3 Thesis outline

This thesis compiles four different studies, which investigate biocolorant applications in wood coatings, thermoplastics, and anodized aluminum. Three of these studies are published as research articles, whilst the fourth study is original to this thesis. The studies can be summarized as follows:

Indigo biocolorant obtained from *Isatis tinctoria* was used as a pigment for commercial linseed oil-based wood coatings in **Publication I**. Durability of the biocolored coatings was assessed by artificial weathering test, which emulates long-term exposure to degrading outdoor conditions, such as rain, humidity, and sunlight. The study showed that wood coatings pigmented with natural indigo presented higher color stability and weathering resistance compared to unpigmented coatings or coatings using commercial ultramarine pigment. However, coatings employing synthetic indigo substantially outperformed the coatings with natural indigo. Additionally, increased degradation rate of indigo pigments was observed in the paint-based coatings due to photocatalytic effect caused by titanium dioxide in the paint formulation.

The indigo pigment from *Isatis tinctoria* was used again in **Publication II**, where a novel purification method for natural indigo was introduced and viability of the purified natural indigo pigment for polypropylene (PP) coloration was investigated. The purified pigment was mixed into PP matrix via extrusion, after which 3D-printing was utilized to form biocolored PP specimens. Furthermore, color stability of the biocolored specimens and DMSO solutions of purified pigment were determined with a lightfastness test under Xenon arc light. The results showed that purification of natural indigo successfully decreased the amount of impurities in the pigment and improved its lightfastness properties in PP matrix. Nevertheless, despite the improved stability and color intensity achieved by purification, the purified natural indigo pigment remained substantially less stable compared to synthetic indigo pigment.

Inspired by the previous work with PP, the aim of **Publication III** was to find suitable biocolorants for polylactic acid (PLA) coloration. Optimally, the biocolorants would provide good color quality, be suitable for large-scale coloration, and protect PLA from photodegradation without negatively affecting mechanical properties of PLA. Thus, biochar and kraft lignin biocolorants from forest industry residues and dried biocolorant extracts from *Isatis tinctoria*, *Rubia tinctorum*, and *Reseda luteola* dye plants were selected for the study. The biocolorants were mixed with PLA via extrusion and injection molded into plastic rods, which were subjected to tensile test and lightfastness test. As a result, good color quality and lightfastness performance was achieved with most biocolorants. Moreover, all biocolorants substantially improved photodegradation resistance of PLA. The best photodegradation resistance was achieved with kraft lignin biocolorant, which also enhanced the tensile properties of PLA and presented good lightfastness.

To broaden the selection of engineering materials, a previously unpublished experimental study on paint-free biocoloration of aluminum is included in this thesis. The aim of the study was to investigate biocoloration of anodized aluminum with *Rubia tinctorum* and *Reseda luteola* extracts. The anodization was done in an electrolytic solution, where direct current was applied between two aluminum specimens. The current induced an electrochemical oxidation reaction on the surface of the anodic specimen, forming a thin and porous aluminum oxide layer. After forming the aluminum oxide layer, the anodized specimen was submerged and kept in biocolorant solution, allowing the biocolorant molecules to interact with the porous oxide layer. Due to weak electrostatic forces and coordination interactions between biocolorant molecules and the porous structure, the biocolorant molecules diffused into the nano-sized pores. Finally, the pores were hydration sealed by submerging the anodized specimen in boiling water. The resulting biocolored specimens presented even and intense metallic colors but only showed a moderate lightfastness performance.

2. Background

2.1 Origin of color

Humans perceive color when electromagnetic radiation in wavelength range of 400 nm – 700 nm, commonly known as visible light, triggers up to one of the three types of photosensitive cone cells in our retinas.[37–41] Each cone cell type responds to slightly different wavelengths by sending a neural impulse to our brain, which compiles the information from numerous cone cells and transforms it to a color sensation.[42, 43] Because most objects do not emit visible light, we perceive color of an object based on external light reflecting from its molecular structure.[44] Thus, for any non-radiating object, color is not an intrinsic property only defined by its molecular structure but a variable parameter which also depends on illumination around the object.[44, 45] For instance, a flower in direct sunlight exhibits substantially different color than the same flower under a cloudy sky or in bare moonlight at night.[46] However, assisted by the fact that most light sources contain all wavelengths of visible light, our brains are accustomed to varying illumination and thus tend to perceive color as a static attribute of a material.[47–49]

To explain how all materials produce different colors under constant illumination conditions, Witt's color theory proposes association between non-grayscale colors and specific molecular functional groups called chromophores and auxochromes.[37] Chromophores, such as azo (-N=N-) group in methyl orange dye or carbonyl (-C=O) groups in alizarin, absorb certain wavelengths of visible light particularly well and act as main producers of color.[37] Auxochromes, such as sulphonate (-SO3H) group in methyl orange or hydroxyl (-OH) groups in alizarin, complement chromophores by modifying the intensity or location of their wavelength absorption bands.[50–52] For a molecule to produce a non-grayscale color, it either requires several conjugated chromophores or a chromophore accompanied by an auxochrome in its structure.[37, 53, 54] Despite being a generalized depiction of complex light absorption mechanics, almost all dyes and pigments contain chromophoric groups as described in Witt's theory.[37] As it stands, Witt's theory is still used in color science especially for developing new dyes and pigments.

In practice, colors are often determined using a reflectance spectrophotometer, which collects light reflected from an object and measures its wavelength-specific intensity across visible spectrum.[55–59] To convert the reflectance data to match human interpretation of color, various mathematical models can be used to present the spectral reflectance data as a single point in a coordinate system.[60–62] For instance, the CIELab color model used in this thesis presents individual colors in a coordinate space defined by three opposing color pairs: black-to-white parameter L^*, green-to-red parameter a^* and blue-to-yellow parameter b^*.[59, 60]

2.2 Color fastness

Color fastness is an umbrella term for various properties related to material's ability to retain its color when exposed to external stress, such as light, water or mechanical wear.[55, 63–65] All colored materials require different color fastness properties depending on their intended use.[66, 67] For instance, a pigment used in house paint must have excellent lightfastness due to direct sunlight exposure. On the other hand, lightfastness is less relevant to a bath towel, which requires good wash fastness instead. Regardless of application, adequate color fastness properties are paramount to ensure sustainable life cycle of a colored object.[68] Products related to fashion or decoration are often picked for their vibrant colors, and even the slightest fading may lead to discarding the old product for a new one.[66, 69, 70] Furthermore, people tend to dislike fully functional items with faded colors even when the items are not fashion-related in the first place.[71]

Considering all forms of color fastness, lightfastness is among the most complex and the most studied properties.[67] Lightfastness refers to ability of a colorant to resist photodegradation, which is to some extent a necessary ability for all colorants.[65, 72] Moreover, colorants are by default susceptible to photodegradation because they are designed to absorb visible wavelengths of electromagnetic radiation.[73, 74] When colorant molecule absorbs energy from radiation, it temporarily ascends to an excited electronic state.[75] To return to the ground electronic state, the colorant molecule must release the absorbed energy in some way.[75] This may initiate degradative photochemical reactions, such as oxidation or reduction, depending on molecular structure of the colorant.[73, 74, 76] Visually, photodegradation of a colorant is observed as color fading, which means that the color of a photodegraded object is perceived as less intense compared to a non-degraded object.[77] The visual difference is created by the decrease in the number of colorant molecules on the surface of the object.[73]

Not light alone, but also other external stressors, such as moisture, heat, or mechanical stress, have their own ways to induce colorant degradation.[67] Thus, to achieve long-lasting colors, various standardized tests have been developed to ensure colorant stability in the most expected conditions.[67, 78] In such tests, the colored objects are subjected to one or more stressors, and any differences in their color before and after exposure are evaluated by visual observation and/or using a reflectance spectrophotometer.[67, 79] These ageing tests are widely implemented in colorant industry to ensure that stable enough colorants are used in colored products, so that the perceived color of the product would remain unchanged throughout its whole life cycle despite the external stressors.[78, 79]

2.3 Biocolorants from cultivated plants

In ancient times, most organic dyes were produced by hot water extraction from wild plants collected from the surrounding natural environment.[27] Despite the multitude of available species, the early dyers discovered that red and blue dyes of good quality could only be obtained from few scarcely available dye plants, such as *Rubia* and *Indigofera* species.[26, 80] In contrast, decent yellow dyes could be extracted from numerous species.[26, 81] Nevertheless, most of the yellow dyes were prone to fading, and the species producing relatively stable yellow dyes became highly valued.[81] Due to limited access to high-value dyes, increasing knowledge about the most potent dye plants eventually led to intentional cultivation of those species over time.

As mentioned in the introduction, agricultural cultivation of biocolorants was almost completely halted by the rapid development of synthetic colorants in the late 19th century.[27] Compared to biocolorants, the synthetic colorants showed broader color palette, brighter shades, better color stability, more consistent quality, and cheaper market prices.[82] However, the raw materials for synthetic dyes are derived from petroleum and their syntheses use multiple hazardous chemicals.[9, 10] Even though modern biocolorant cultivation still requires more arable land, water, and manual labor than synthetic colorant production, various life cycle analysis studies have shown that environmental footprint of a cultivated biocolorant is in many cases smaller than footprint of a comparable synthetic colorant.[83] Moreover, various dye plants have shown to improve soil fertility when they are included in crop rotation. However, considering substantial land use requirements of both biocolorant cultivation and the current food production system, it is impossible to fully replace synthetic colorant production by agricultural means only.[84, 85] Nonetheless, agricultural cultivation of biocolorants can certainly be viewed as part of the solution to considerably reduce environmental impacts of colorant production.[86]

In European climate, four dye plant species, woad (*Isatis tinctoria*), ai (*Polygonum tinctorium*), madder (*Rubia tinctorum*), and weld (*Reseda luteola*), were extensively cultivated before the industrial revolution.[87] Blue colors were produced with indigo from either woad or ai leaves, red colors were produced from anthraquinone-class alizarin dye from madder roots, and yellow colors were produced with flavonoid-class luteolin dye extracted from weld biomass.[87] Even though woad, madder, and weld are still cultivated in Europe as plant-based sources of indigo, alizarin, and luteolin dyes, the scale of cultivation is relatively small.[87–89] Due to the growth potential in production of plant-based indigo, alizarin, and luteolin in Europe, more detailed discussion of sources and properties of these biocolorants is presented in the following subsections.

2.3.1 Indigo

Indigo (indigotin) is a blue dye, which has been used since ancient times.[26] The traditional way to produce indigo is to extract it from leaves of specific plant species, most commonly *Indigofera sp* in tropical climates and *Isatis tinctoria* or *Polygonum tinctorium* in temperate climates.[90] Before industrial revolution in the 19th century, indigo was highly expensive due to its unique and durable color. After the pathways of indigo synthesis were discovered in the late 1800s, the value of plant-based indigo plummeted and indigo production shifted almost completely from fields to factories.[30, 91] However, contrary to many other natural colorants, indigo was never completely replaced by a different synthetic compound. The synthetically produced indigo colorant, hereafter referred to as synthetic indigo, is still commonly utilized in modern denim dyeing.[92]

In the nature, indigo is only present in the form of its precursors, water-soluble indican and isatan B, which are indoxyl radicals attached to a sugar group.[93] The indigo pigment can be obtained by water extraction of the precursors from indigo plant leaves and detaching the sugar groups from the indoxyl radicals by alkali hydrolysis.[94] This causes the detached indoxyl radicals to react with each other, forming leuco-indigo.[91] After hydrolysis, the indigo pigment can be formed by adding oxygen to the solution, causing an oxidation reaction of leuco-indigo to water-insoluble indigo.[95–97] The oxidation reaction is presented in Figure 1.

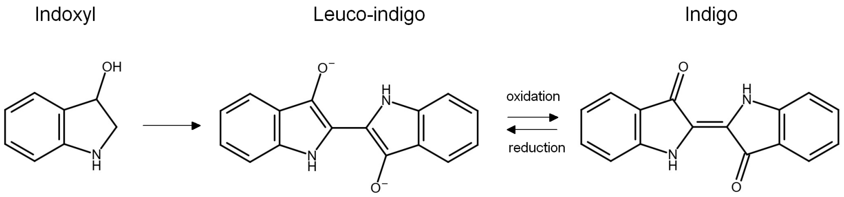

Figure 1. Oxidation of water-soluble indoxyl precursors to solid indigo pigment. Images of the molecular structures were created using Marvin JS by Chemaxon.

Indigo pigment is almost invariably used for textile dyeing.[90] However, due to its insolubility, as specific reduction-based method known as vat dyeing must be used.[98] In vat dyeing, the indigo pigment is first reduced back to the water-soluble leuco-indigo form.[93] The reduction reaction is commonly done in alkaline and mostly anaerobic water solution in presence of a sodium hydrosulfite catalyst.[99–101] When a fibrous fabric is introduced to the leuco-indigo solution, the leuco-indigo molecules will spread amidst the fabric fibers.[91] After the fabric is lifted from the solution, the attached leuco-indigo molecules will come to contact with oxygen and revert to the stable pigment form.[96, 97] During oxidation, some of the newly formed pigment particles are trapped between the fabric fibers, which gives the dyed textile an indigo-blue color with excellent lightfastness.[102] However, due to low affinity between the textile fibers and indigo pigment, most indigo-colored textiles present only low-to-moderate rubbing fastness and wash fastness performances.[91, 102]

Despite its stable molecular structure and exceptional lightfastness properties amongst natural colorants, indigo is nowadays rarely utilized in non-textile applications.[103] Historically, though, indigo pigment was frequently used in blue paints whenever accessible due to its high resistance to fading by light exposure or abrasion.[104–107] Thus, applications of natural indigo in pure pigment form are investigated in the experimental part of this thesis.

2.3.2 Alizarin

Alizarin (1,2-dihydroxy anthraquinone) is an anthraquinone-class red dye, which can be extracted from *Rubiaceae* plant species.[108, 109] The most historically relevant plant-based source of alizarin is madder (*Rubia tinctorum*), which contains alizarin in its roots.[108] Before the discovery of synthetic dyes, alizarin was a valuable and popular choice for fabric dyeing akin to indigo due to its deep red color and better fastness properties compared to other red dyes.[26] In contrast to indigo, however, alizarin was almost completely replaced by other synthetic dyes during the 1900s.[82, 110] Although pure alizarin is nowadays rarely synthesized for coloring purposes, natural alizarin is still produced to some extent via large-scale madder cultivation.[111] The chemical composition of alizarin is presented in Figure 2.

The existing commercial production of alizarin biocolorant and its popularity in the pre-industrial era have attracted many research projects to investigate its potential as a sustainable biocolorant for fabric dyeing.[112] Hitherto, the dyeing studies have generally yielded promising results, including good lightfastness and antimicrobial properties for the dyed fabrics.[113–115] Despite the success, more critical reports have also been published, emphasizing high production costs of alizarin and presenting concerns about its toxicity level in aquatic environment.[86, 116] Nonetheless, less attention has been paid to coloring non-fabric materials with alizarin, even though using alizarin for coloring cosmetics, plastics, and even wood have been studied occasionally. [111, 117, 118]

2.3.3 Luteolin

Luteolin (3′,4′,5,7-tetrahydroxyflavone) is a polyphenolic, flavonoid-class dye, which is present in numerous plant species.[81, 119–121] Such as indigo and alizarin, luteolin is a traditional biocolorant, which was already widely used for textile dyeing before the uprise of synthetic dyes.[26, 122] The main historical source of luteolin was weld (*Reseda luteola*), which was used in dyebaths to obtain yellow and green colors.[26, 123] Similar to madder, mass cultivation of weld was not completely halted after luteolin was replaced by other synthetic compounds with better color fastness properties and more intense colors.[82] Thus, luteolin from weld origin is still commercially available for dyeing, even though luteolin is no more used in industrial scale coloration. The chemical composition of luteolin is shown in Figure 2.

In modern research, luteolin is widely regarded as a highly antioxidative compound with significant potential for anti-cancer, anti-inflammatory, and even anti-viral applications.[120, 121, 124, 125] Thus, studies on luteolin are mostly focused on its biomedical properties rather than biocoloration applications. Nevertheless, biocoloration with plant-based luteolin is still studied, especially in textile dyeing context.[119, 122] Besides the antioxidative properties mentioned earlier, luteolin has shown to improve UV-protective characteristics of certain fabrics.[126] Furthermore, according to some studies, applying various mordants and altering the traditional dyeing methods can be utilized to improve the initially lackluster lightfastness properties of luteolin.[82, 127, 128] In addition to textile dyeing, luteolin biocolorant has been investigated for plastic and food coloration. [111, 129]

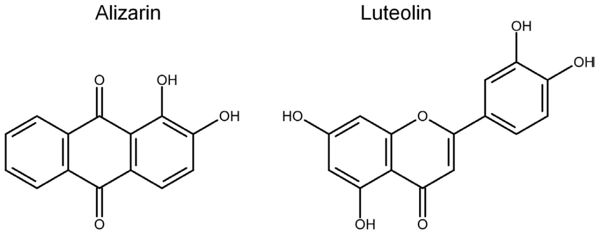

Figure 2. Chemical structures of alizarin and luteolin. Images of the molecular structures were created using Marvin JS by Chemaxon.

2.4 Biocolorants from industrial side streams

Nowadays, numerous industrial processes generate large amounts of organic waste, which is often used for energy or landfill, even though valuable products could be extracted from the waste stream.[84, 130] Notably, to supplement the biocolorant palette from intentionally cultivated plants, microbes, fungi, or algae, a variety of biocolorants can also be acquired from certain industrial side streams.[84] Even though utilizing industrial side streams offers less control over raw material quality compared to intentional cultivation, it broadens the overall selection with many biocolorants that could not be easily acquired via cultivation.[131] Moreover, skipping the cultivation phase can lead to multiple sustainability advantages, such as reduced carbon footprint, water usage, and usage of cultivable land.[86] Furthermore, if a low-value side stream can be utilized in large scale, abundance of the raw material can translate to a low production cost depending on the extraction and purification processes.[86] Even though utilizing industrial side streams for biocolorant production is a relatively novel concept, it has already inspired many research projects due to its innate potential to generate sustainable and economically viable biocolorant production pathways.[132–137] Subsequently, the activities in biocolorant research have already created healthy business segments for novel companies, such as Keracol or Natural Indigo Finland. Although the number of applications investigated in both commercial and non-commercial field is large enough to fill multiple review articles, for the sake of conciseness, only a relatively narrow discussion is presented here.

Recently, the most suitable side streams for colorant production have originated from either food industry or forestry. Regarding food industry, a lot of research has been done to utilize waste streams of various fruit peels, nutshell peels, or onion peels.[84] Onion peels, for instance, are considered a very low-value waste stream; however, they contain substantial amount of flavonoid-class quercetin, which has been used as a biocolorant with promising results.[132] Besides various peels, anthocyanin-rich extracts from pomace of various fruits and berries have also been tried as natural colorants for large-scale production.[130] The general problems with pomace extracts for non-edible applications have been low lightfastness, high amount of sugars in the extracted colorant, and competing use cases for the pomace especially in the superfood segment.[138] Despite these obstacles, many successful textile dyeing trials have been done with pomaces-based biocolorants, for example, anthocyanin biocolorant extracted from chokeberry pomace.[139] The third major upcoming segment from the food industry are biocolorants extracted from residual coffee and tea waste.[84] The tea waste contains high amounts of polyphenolic colorants, especially tannins, which have been tested both as a biocolorant or as a bio-based mordant.[135, 140, 141] Coffee, in turn, contains melanoidin, which is a polymeric molecule consisting of sugars and amino acids.[136] Consumer products dyed with both tea and coffee-based colorants are already on their way to the market, but academic research regarding both colorants is still frequently being carried out.[142–146]

Forest industry biocolorants are somewhat limited in their color palette, but their potential lies in very low value and large volume of the generated waste.[137, 147] The most common biocolorant sources among forest industry waste streams are various tree bark extracts, lignin-based colorants, and biochar.[35, 148–152] Similar to the tea waste extracts, the most prevalent biocolorants in wood bark extracts are different types of tannins.[153, 154] Even though the tree barks often contain undesirable inorganics, the available volume of tree bark waste is significantly higher than that of tea waste, which likely equals higher scale-up potential after the optimized extraction processes are found.[155, 156]

In addition to producing high amount of waste, production plant infrastructures in forest industry segment are often built to support addition of large-scale chemical operations by default, which can generate local biocolorant value chains.[86] For instance, processing of two different pulp mill waste streams, black liquor and wood chips, into dried kraft lignin powder and biochar powder, can already be done locally in large scale.[157–161] Since both kraft lignin and biochar are both highly relevant to the experimental part of this thesis, their properties, applications, and origins are discussed separately in the following subsections.

2.4.1 Kraft lignin

Kraft lignin is a heterogenous and amorphous polymer with a branching molecular structure, which consists of phenolic monomer groups linked by mainly ether and C–C bonds.[162–164] The intramolecular bonds in kraft lignin are strong, which results to a relatively stable molecular structure.[162] Furthermore, kraft lignin contains high amounts of polar hydroxyl groups, which keeps its structure compact due to formation of weak hydrogen bonds between the branches.[165–167]

Every year, approximately 70 million tons of kraft lignin is generated as a byproduct in pulp and paper industry, where kraft process is utilized to separate lignin, hemicelluloses, and other extractives from lignocellulosic biomass.[168–170] The residual stream containing kraft lignin, commonly known as black liquor, is almost invariably burned for energy owing to its high calorific value.[171, 172] However, due to substantial volume of the residual lignin, possibilities to use it for applications beyond energy production have been extensively investigated in the past years.[170, 173, 174] Consequently, multiple potential large-scale applications for kraft lignin have been found, for instance, using it as a filler for thermoplastics or as an ingredient in glues or adhesives.[168, 175, 176] Moreover, studies about using kraft lignin as a biocolorant have been conducted as well, showing that kraft lignin colorant possesses good lightfastness, rubbing fastness, and UV protective properties, although its color palette is currently limited to a range of brownish shades.[177–179]

2.4.2 Biochar

Biochar is a residual mixture of carbon and inorganic compounds obtained by pyrolyzing organic matter in oxygen-free conditions at high temperature.[180, 181] Its composition and structure both depend on pyrolysis temperature and contents of the organic raw biomass.[180–182] Biochar presents a deep black and highly matte color due to its porous structure and high carbon content.[181] For most applications, biochar is ground into suitable particle size and used as a coarse or fine powder depending on its use.[182–185]

Biochar is not directly present in any industrial side streams, however, almost any organic matter can be turned to biochar by pyrolysis.[186] Thus, due to abundant raw materials and unique properties of biochar, its potential applications have been heavily investigated.[187] The investigations have shown, for instance, that biochar can be effectively used for soil and water remediation, electrochemical cells, and catalytic materials.[186, 188–191] Furthermore, using biochar as a filler in various engineering materials has yielded promising results.[192–196] Some trials of using biochar as a black biocolorant have also been conducted, for example, biochar has been used to replace black pigment in printing inks and various polymer matrices.[148, 185, 197–199] The studies have shown that coloring properties of biochar are in many cases comparable to commercial black pigments and that biochar may also improve mechanical properties of the colored matrices when used for polymer coloration.[148, 197, 198] Moreover, biochar pigment has shown reduced carbon footprint compared to the commercial pigments in life cycle analysis.[185]

2.5 Biocolorants in engineering materials

Engineering material is a phrase commonly used to describe a large group of human-manufactured solid materials, which are frequently used in structural and/or mechanical applications.[200–202] The exact boundaries between engineering and non-engineering materials may vary slightly depending on the definition.[201] However, it is mostly agreed that all engineering materials belong to one of these categories: metals, polymers, ceramics, and composites, including naturally occurring composites such as wood.[201] In contrast to textiles, cosmetics, and food, published research rarely mentions engineering materials as a potential application field for biocolorants.[86, 203, 204] The emerging studies on biocoloration of engineering materials explore applying biocolorants to wooden materials, wood coatings, or thermoplastics.[19, 111, 205–208]

The two main methods for applying biocolorants to wooden materials are coating and dye impregnation, of which the coating option has been investigated much more frequently due to having many existing applications with synthetic colorants.[208] The colored wood coatings, such as paints, varnishes, lacquers, or stains, are widely applied on both interior and exterior wood in built environment.[209–212] In its most basic form, a colored wood coating consists of an organic solvent base, a binder fraction, various additives, and a fine pigment powder as a colorant.[213] Due to the presence of binder fraction, colorants in wood coatings are used as solid pigments that do not attach to the wooden surfaces with chemical bonds.[213] Thus, any biocolorant that can be brought to a relatively inert pigment form, could theoretically replace a synthetic colorant in any wood coating formulation.[208] However, in exterior coatings, the pigments must be highly resistant to ultraviolet light and moisture, which limits the practical biocolorant choices.[214] Nevertheless, recent experiments with exterior wood coatings have proved that certain biocolorants, such as tannin-rich tree bark extracts, can improve weathering resistance of the coating matrices.[215, 216]

Different from wood coloration, thermoplastic coloration is frequently done using both solid pigments and soluble dyes.[205] Moreover, instead of coating the plastic, the colorants are often added to molten plastic and then injection molded or extruded into colored solid objects.[205] As a result, the colorant is trapped inside the plastic matrix and coloring it without requiring further treatment.[217] To achieve a uniform and stable color, the main requirements for plastic colorants are high heat stability, good lightfastness, and ability to resist certain chemicals.[218] Additionally, if a pigment is used, the particle size should generally be below 30 µm to ensure color uniformity.[218, 219] Even though many biocolorants fulfill the aforementioned requirements, upscalable biocoloration processes for plastics is rarely studied.[205] Nevertheless, a few studies have still been conducted, for instance, PLA biocoloration with almond shells, walnut husks, various plant extracts, and spent coffee grounds has been investigated.[111, 205, 220–223] Other thermoplastics have been studied as well, such as PP, polyvinyl chloride (PVC), and polymethyl methacrylate (PMMA).[224, 225] In these studies, examination of long-term durability properties showed that although many biocolored plastics are only suited for decorative and/or short-term applications, the indigoid- and anthraquinone-colored plastics achieved sufficient color stability for long-term applications when covered from direct sunlight.[224, 225]

Metallic materials are most often colored by applying a corrosion resistant coating layer, such as paint, conversion coating, or different metallic material.[226] Among these coating types, paints are the only ones to contain colorants themselves, even though certain colorant can be applied to the conversion coatings afterwards. Similar to wood coatings, paint coatings for metals often include the four basic fractions: organic solvent, binder, colorant, and additives.[226] In terms of colorant addition and requirements, similar principles can be applied in biocoloration of both wooden and metallic surfaces.

Opposed to paint coatings, conversion coatings are formed on the metallic surface by inducing chemical reactions, such as oxidation, on surface layer of the metallic material.[226] For instance, aluminum can be coated via anodization process, which utilizes electrochemical oxidation to form a porous oxide layer on the aluminum surface.[226] Due to the porous nature of the aluminum oxide layer, it acts as a trap for certain types of dye molecules when submerged in a liquid dyebath. Thus, applying a colorant on an anodized surface does not require any binders, plasticizers, or mordants to attach the colorant to the oxide layer. Typically, the colored aluminum oxide layer has thickness less than 25 µm, is somewhat resistant to abrasion, and presents a glossy, metallic color. Moreover, multiple studies have shown that the thin oxide layer substantially improves corrosion resistance and microhardness properties of aluminum surface.[227–230]

Dyed anodized aluminum is commonly used in household electronics, sporting goods, and engineering components, for instance, but few studies can be found on dyeing anodized aluminum with biocolorants. Some studies have still been conducted on the matter, for instance, a carotenoid-type crocin biocolorant has been tried for electrolytic coloration of anodized aluminum in 1989.[231] However, no distinctive color from crocin was achieved on anodized surfaces, but a decorative greenish layer was obtained for non-anodized aluminum instead. Despite the discouraging conclusions with crocin, more recent studies from Indonesia have obtained promising results with food processing residues for dyeing anodized aluminum.[232–235] Notably, encouraging results were achieved with curcumin dye, which presented bright, mostly even colors with improved wear resistance on the aluminum oxide layer.[235] Moreover, bright shades have been obtained using chlorophyll-containing extracts from *Pandanus amaryllifolius* leaves and anthocyanin-containing extracts from either purple sweet potato waste or mangosteen peels, even though further research is needed to achieve more uniform coloration.[233, 234] Finally, dyeing anodized aluminum with anthocyanin-containing extracts from purple cabbage and dragon fruit peel have been tried, although red and purple food colorants were used as assisting dyes.[232] Even though deep shades ranging from purple to orange were obtained, poor color uniformity and requirement for an auxiliary colorant make the results less promising compared to the studies where only natural dyes were applied.[232–235]

3. Experimental

The materials and methods used for biocoloration of engineering materials are described in this chapter. Moreover, methods for testing and evaluating color fastness, colorant degradation, and mechanical properties of the biocolored samples are briefly described. For the sake of clarity, only essential information is presented; exact details of the materials and methods used in the experiments can be found in the corresponding **Publications I–III**.

3.1 Materials

3.1.1 Engineering materials

Planed pine wood panels were purchased from a local hardware store and used as a base material for wood coatings in **Publication I**. Prior to applying any coatings, the panels were cut to a size of 15 x 70 x 320 mm and carefully hand sanded with mesh 150 sanding paper according to the SFS-EN 927–6:2018 accelerated weathering standard. Virgin PP powder with maximum particle size of 90 µm and melting temperature of 159–171 °C was purchased from Goonvean Fibres Ltd and used in the **Publication II**. Prior to any experiments, the powder was stored at room temperature in closed storage with desiccant crystals. Virgin PLA granules of injection molding grade with molecular weight of 116000 g/mol and melting temperature of 145–160 °C were purchased from NatureWorks LLC and used in **Publication III**. Aluminum bars of 6082 grade used in the experiments presented in **Chapter 4.5** were purchased from a local machinery shop. Prior to any experiments, the aluminum bars were scrubbed with a damp cloth, thoroughly rinsed with ion-exchanged water, dried, and carefully wiped using a cloth soaked with ethanol to remove any possible contaminants on the aluminum surface.

3.1.2 Biocolorants

The bio-based indigo, also referred to as natural indigo in this thesis, was obtained as a dried pigment from Natural Indigo Finland Ltd and used to produce blue colors in **Publications I**, **II**, and **III**. The original production pathway for the obtained pigment involved large-scale agricultural cultivation of woad (*Isatis Tinctoria*), water extraction of indigo precursors from the harvested *Isatis* leaves, and conversion of the extracted indigo precursors to the pigment form via oxidation. Dried water-ethanol extracts of madder (*Rubia tinctorum*) and weld (*Reseda luteola*) used in **Publication III** and in the experiments presented in **Chapter 4.5** to produce red and yellow hues were obtained from Greening Ltd. Kraft lignin (BioPiva™) used as a brown pigment in **Publication III** was purchased from UPM-Kymmene Ltd. Finally, biochar used in **Publication III** as a black pigment was obtained from Häme University of Applied Sciences. The biochar pigment was produced from 1:1 mixture of *Alnus incana* and *Betula pendula* wood chips via pyrolysis. The wood chips were pyrolyzed in oxygen-limited atmosphere at 600 °C temperature for 20 minutes, after which the obtained biochar was ground to coarse powder and dried overnight in 55 °C temperature.

3.1.3 Other materials

To determine accelerated weathering performance of natural indigo pigment in authentic wood coating matrices in **Publication I**, linseed oil-based thinner, primer, varnish and paint were obtained. Uula Universal Thinner (UT), Uula Exterior Primer (EP), Uula Boat Varnish (BV), and Uula Linseed Oil Paint (LOP) were all purchased from Uula Color Ltd. UT was dearomatized and hydrotreated heavy naphtha, which contained 35 w-% of boiled linseed oil and 65 w-% other dearomatized hydrocarbons. The resulting UT composition was a mixture of C10-C13 hydrocarbon isomers (n-alkanes, isoalkanes, and cyclics) with less than 2 % aromatic compounds. Main constituents of both EP and LOP were boiled linseed oil, UT, and TiO_2 pigment. BV consisted of boiled linseed oil, UT, and bio-based resins. Previous literature reports have shown that the boiled linseed oil, which was the main component of EP, BV, and LOP, contains approximately 45–65 % linolenic acid, 13–25 % oleic acid, 10–20 % linoleic acid, 3–10 % palmitic acid, and 1–6 % stearic acid.[236–238]

Synthetic indigo pigment powder of MQ200 grade was obtained from Sigma-Aldrich Ltd and used as a reference colorant in **Publications I** and **II**. Another colorant used as a reference in **Publication I**, Pigment Blue 29, was purchased in powder form from Uula Color Ltd. Dimethyl sulfoxide (DMSO) used as a solvent for indigo pigments in **Publication II** was purchased from Aquarius Pro Life Ltd. Hydrochloric acid solution (37 w-%) from Sigma-Aldrich Ltd diluted to 2M concentration was used for purifying bio-based indigo pigment in **Publications II** and **III**. In the experiments presented in **Chapter 4.5**, sulfuric acid solution (96 w-%) from Sigma-Aldrich Ltd diluted to 2M concentration was utilized as a medium liquid for electrochemical anodization process. Finally, sodium hydroxide pellets (≥98 % purity) dissolved to distilled water in 1M concentration and laboratory grade ethanol (95 w-%), both from Sigma-Aldrich Ltd, were used to prepare aluminum bars for anodization experiments presented in **Chapter 4.5**.

3.2 Methods

3.2.1 Colorant preparation

Natural indigo pigment used in **Publications I**, **II** and **III** and synthetic indigo pigment used in **Publications I** and **II** were prepared by grinding them in a planetary ball mill (Fritsch Pulverisette 6 with ZrO_2 shell and balls). The grinding process was done in 60-second periods at rotational speed of 550 rpm and repeated 10 times in total. The HCl-purified natural indigo pigment for **Publications II** and **III** was prepared from the ball-milled natural indigo powder by soaking 10.00 g of the pigment in 2M hydrochloric acid for 24 hours in room temperature. After soaking, the solid pigment phase was separated from the liquid HCl phase by centrifuging. The purified pigment was then washed 4 times by mixing it with distilled water and separating the solid and liquid phases with a centrifuge. Post-washing, the pigment was dried in 50 °C for 24 hours and ground into fine powder with IKA A 10 basic batch mill, resulting in 5.12 g of dry pigment. Biochar and kraft lignin used in **Publication III** and pre-dried madder and weld extracts used in **Publication III** and in the experiments presented in **Chapter 4.5** were prepared by drying and grinding akin to the HCl-purified natural indigo after its purification process.

3.2.2 Preparation of color-coated wooden panels

To create biocolored versions of existing paint and varnish coating products in **Publication I**, natural indigo pigment was manually mixed with linseed oil-based BV and LOP. Furthermore, reference coatings colored with synthetic indigo and Pigment Blue 29 were mixed in the same manner. Notably, 5 w-% of UT was added to all colored coatings to neutralize the increase in viscosity caused by colorant addition. The resulting BV-based coating formulations contained 5 w-% of colorant, 5 w-% of UT and 90 w-% of BV. For LOP-based formulations, different amount of each colorant was used to obtain coatings with matching color intensity. Thus, the resulting LOP-based coatings contained 5–20 w-% of colorant, 5 w-% of thinner and 75–90 w-% of LOP.

Four coating layers in total were manually applied on each wooden specimen. First the specimens were primed with two layers of EP to ensure good adhesion of the exterior coating. Then, two layers of either BV-based or LOP-based coating were applied on top of the previous layers. After applying each coating layer, the specimens were dried in room temperature for 48 hours. As a result, four different specimens of both BV-based and LOP-based coatings were obtained: one specimen for each colorant and one uncolored specimen.

3.2.3 Preparation of indigo-colored polypropylene rods

The PP specimen rods in **Publication II** were made from pre-dried mixtures of PP powder and indigo pigments. Four different PP-indigo mixtures were prepared: two with 0.25 w-% and 0.50 w-% of unpurified natural indigo, one with 0.25 w-% of HCl-purified natural indigo, and one with 0.25 w-% of synthetic indigo. The mixtures were blended and extruded into monofilaments with a twin-screw extruder at 200 °C temperature and cooled on a belt conveyor. In addition to the colored filaments, an uncolored filament with pure PP was extruded in the same manner. The filaments were then 3D-printed to 50 x 10 x 2 mm specimen rods using a custom PP printing base to minimize undesired warping or dislocation effects.

3.2.4 Preparation of biocolored polylactic acid rods

The PLA specimen rods in **Publication III** were prepared by mixing virgin PLA granules with 0.1 w-% of five different biocolorant powders: HCl-purified natural indigo, madder extract, weld extract, biochar, and kraft lignin. The mixtures were blended together inside an injection screw at 145–165 °C barrel temperature and injection molded to 165.0 mm long, 12.8–19.0 mm wide and 3.0 mm thick dogbone-shaped specimen rods. Exact dimensions of the specimens are described in ASTM D638 tensile test standard under Type I specimen category.

3.2.5 Preparation of biocolored anodized aluminum

Dyebath preparation

In the experiments presented in **Chapter 4.5**, six separate dyebaths for dyeing anodized aluminum were prepared from 1.0 w-% water solutions of madder extract and weld extract. Both colorants were used to make three dyebaths with pH-values of 5.0, 6.5, and 8.5. The target pH-value for each dyebath was achieved by addition of either 1M hydrochloric acid or 1M sodium chloride solution.

Anodizing process

In the experiments presented in **Chapter 4.5**, aluminum specimens were anodized electrochemically and biocolored with madder extract and weld extract. A pre-cleaned aluminum specimen was etched by soaking it in 1M sodium chloride for 60 seconds and thoroughly rinsed with ion-exchanged water immediately after etching. After rinsing, the specimen was partially immersed in 2M sulfuric acid bath together with a sheet of pre-cleaned aluminum foil. The specimen and the foil were carefully separated from each other and connected to the same power supply; the specimen to the positive terminal to act as an anode and the foil to the negative terminal to act as a cathode. Then, the power supply was switched on, which induced an electrochemical oxidation reaction on the surface of the anode forming a porous aluminum oxide layer. Current and voltage between the anode and the cathode were kept at 0.13 A and 10.0 V, respectively. After 20 minutes of anodizing, the specimen was detached from the power supply, rinsed with ion-exchanged water, and partially immersed in a dyebath. The dyebath was kept at 60–65 °C temperature and stirred continuously. After 15 minutes, the specimen was removed from the dyebath and submerged in boiling deionized water for 5 minutes.

3.2.6 Aging of the biocolored specimens

Accelerated weathering test

Accelerated weathering according to ISO EN 927-6:2018 was used to simulate outdoor conditions to determine color stability of wood coatings in **Publication I**. The accelerated weathering was done inside a QUV Accelerated Weathering Tester (Q-Lab Corporation Ltd). A single exposure cycle consisted of 24 hours of water condensation in 45 °C temperature, followed by 144 hours of alternating periods of UVA light radiation (0.89 W/m^2nm at 340 nm, 60 °C) for 2.5 hours and deionized water spray (6 L/min) for 0.5 hours. The full exposure cycle was continued for 40 days, resulting in 5.7 exposure cycles in total.

Xenon arc light exposure

In **Publications II** and **III**, color fastness of thermoplastic specimens against prolonged exposure to indoor lighting conditions was simulated according to exposure cycle A1 presented in ISO 105-B02:2014 lightfastness test standard. The lightfastness tests were done in Heraeus Suntest CPS+ weathering chamber under a Xenon arc lamp in 50 °C temperature for 168 hours in total. Importantly, a standard set of eight different blue wool fabrics with known lightfastness were exposed alongside the specimens and used as references for visual lightfastness evaluation. In the experiments presented in **Chapter 4.5**, identical conditions but a shorter test time of 24 hours was used for lightfastness testing of biocolored anodized aluminum specimens. Additionally, in **Publication II**, indigo-DMSO solutions with 1:200000 mixing ratio were exposed to the same conditions for 5, 15, and 30 minutes to determine their color stability against Xenon light exposure.

3.2.7 Visual and microscopic characterization

Visual lightfastness evaluation

In **Publications II** and **III**, lightfastness performance of the light-exposed plastic specimens was visually evaluated according to ISO 105-B02:2014 standard. The color difference between exposed and unexposed specimens was visually compared to color differences of eight partially exposed blue wool fabrics with predetermined lightfastness. Based on the visual evaluation of similarity in color difference, each specimen was matched with one of the eight blue wool specimens given a corresponding lightfastness rating between 1 and 8.

Microscopic characterization
In **Publication III** and in the experiments presented in **Chapter 4.5**, the samples were photographed using an optical microscope. In **Publication III**, the microscopic images were processed with ImageJ software to approximate particle size distribution of the biocolorant inside PLA matrix. Furthermore, in **Publication III** and in the experiments presented in **Chapter 4.5**, scanning electron microscopy (SEM) images were taken to acquire information about surface properties of the specimens.

3.2.8 Spectral characterization

Reflectance spectroscopy
In **Publications I**, **II**, **III**, and in the experiments presented in **Chapter 4.5**, spectral reflectance of the wooden, plastic, and aluminum specimens in 360–700 nm wavelength range was measured with a Datacolor 600 reflectance spectrophotometer. Furthermore, the spectrophotometer was used to convert the spectral reflectance values into CIELab colorimetric lightness parameter L^*, green-red parameter a^*, and blue-yellow parameter b^* to represent of visual color of the measured specimen. Moreover, in **Publication II**, K/S values representing color intensity of specimens were calculated from the spectral reflectance data.

Hyperspectral imaging
In **Publications I**, **II**, and **III**, hyperspectral imaging (HSI) of the solid specimens in 700–1000 nm wavelength range was performed with a Specim IQ portable hyperspectral camera. First, the specimen was cleaned and placed on a flat surface next to a white reference tile. The camera was then placed above the specimen perpendicular to its surface. Moreover, two halogen light sources were placed on opposite sides of the specimen and directed at the specimen surface in a 45-degree angle to avoid specular reflection. After imaging, the spectral data was corrected against the white reference and the average spectrum was calculated from a selected area of 100 x 100 pixels.

UV-Vis spectroscopy
In **Publication II**, UV-vis absorption spectroscopy was used to assess light-induced colorant degradation in the indigo-DMSO solutions. The absorbance spectra of the colored solutions after 0, 5, 15, and 30 minutes of Xenon arc light exposure were measured with a Shimadzu UV-1800 spectrophotometer. Pure DMSO was used as a baseline for all measurements.

ATR-FTIR spectroscopy
In **Publication I**, attenuated total reflection Fourier-transform infrared (ATR-FTIR) spectra of the coatings before and after accelerated weathering was measured using a Bruker Alpha FTIR spectrometer with Eco-ATR sampling module. In

Publications II and **III**, equivalent measurements were performed using a Shimadzu IRSpirit FTIR spectrometer with QATR-S sampling module.

3.2.9 Other methods

In **Publications II** and **III**, thermogravimetric analysis (TGA) of the colorant powders was carried out using Pyris 1 thermogravimetric analyzer. In **Publication III**, tensile properties of PLA specimens were measured with a ZwickRoell tensile testing apparatus according to ASTM D638 standard.

4. Results and Discussion

This chapter summarizes the main findings in **Publications I**, **II**, and **III**. Furthermore, preliminary results of a novel biocolorant study conducted by the author are presented and discussed.

4.1 Biocolorants

The experimental studies in this thesis utilized five different biocolorants: indigo pigment from *Isatis tinctoria* extract, dried madder extract from *Rubia tinctorum*, dried weld extract from *Reseda luteola*, biochar from pyrolyzed mixture of *Alnus incana* and *Betula pendula* biomass, and residual kraft lignin from industrial pulping process. The indigo biocolorant was applied in two forms; an untreated commercial pigment was used in **Publications I** and **II**, whereas a HCl-purified version of the commercial pigment was utilized in **Publications II** and **III**. When dissolved in DMSO in equal concentration, both indigo pigments had comparable absorption spectra with peak maxima at 290 nm and 620 nm as shown in Figure 3. However, compared to the unpurified pigment, peak intensity of the HCl-purified pigment was 3.0 times higher at 290 nm and 2.8 times higher at 620 nm, indicating more intense color and higher pigment purity.

Furthermore, photostability of the dissolved pigments was determined from decreasing intensity of the absorbance peaks during Xenon light exposure. The spectral changes during Xenon light exposure presented in Figure 3 illustrate that both natural indigo pigments had relatively lower absorbance retention (10 – 11 %) than the synthetic indigo pigment (26 %). Notably, despite the higher initial absorbance in HCl-purified indigo, both natural pigments presented similar rate of photodegradation. Thus, the HCl-purification only increased spectral intensity of the pigment but did not affect its photostability.

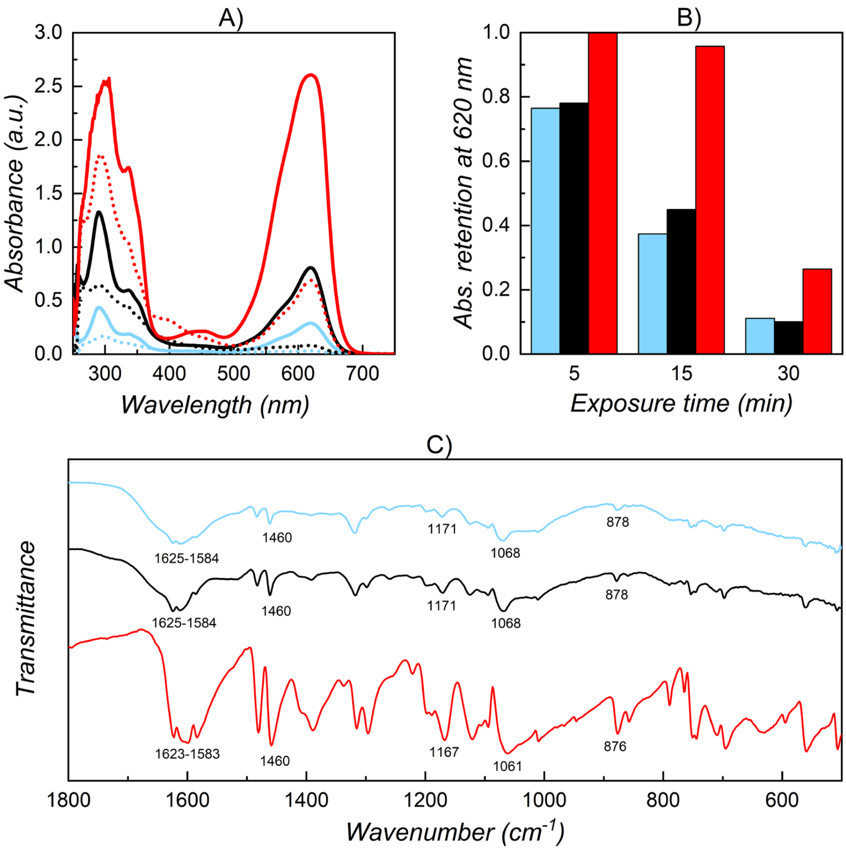

Figure 3. A) Absorbance spectra of indigo pigment solutions before and after 30 minutes of Xenon light exposure. **B)** Absorbance retention at 620 nm over exposure time. **C)** ATR-FTIR spectra of the indigo pigment powders. Color coding of the powders: light blue = unpurified natural indigo, black = HCl-purified natural indigo, and red = synthetic indigo. Reproduced from **Publication II** with permission from Emerald Publishing Group.

The difference in pigment purity was further investigated with TGA. Due to full decomposition of the indigo pigments at the final temperature of 700 °C, the weight percentage of inorganic impurities in the pigments was determined based on the residual mass remaining after heating. The TGA showed approximately 21 w-% impurity content for the HCl-purified pigment and 32 w-% impurity content for the unpurified pigment. Nevertheless, compared to the HCl-purified pigment, the commercial synthetic indigo used as a reference pigment showed approximately 3.2 times higher absorption maximum at 620 nm and presented only 2 w-% impurity content according to the TGA measurement. Supporting evidence for the decreased impurity content was achieved from the ATR-FTIR analysis of the indigo pigments. As presented in Table 1, identical locations for the main IR peaks were detected in the natural indigo pigments. Both pigment powders presented characteristic C=O bands for indigo around 1600 cm^{-1}, C-C stretching vibrational band at 1460 cm^{-1} and the pentagonal ring structure stretching bands at 878 cm^{-1}, 1068 cm^{-1}, and 1171

cm^{-1}.[239, 240] In comparison, minor differences in peak locations were observed in the synthetic indigo pigment, which presented its ring structure peaks at 876 cm^{-1}, 1061 cm^{-1}, and 1167 cm^{-1}.

Table 1. Main IR peak locations of the natural indigo pigments.

Functional group	**Wavenumber (cm^{-1})**
C=O	1609
C–H	1460
pentagonal ring structure	878, 1068, 1171

As seen in a previous study, the impurities in woad-based natural indigo can be observed by shrinkage of the band at 1460 cm^{-1} relative to the broad band at 1609 cm^{-1}.[239] As expected, the most intense IR peaks at 1460 cm^{-1} relative to the band at 1609 cm^{-1} were observed in the synthetic indigo pigment followed by the HCl-purified indigo. The lower peak intensity in the natural indigo pigments is likely caused by the metallic impurities, which can exhibit broad interfering absorbance bands in the 1000–1800 cm^{-1} wavenumber range.[239] In summary, the observations about identical peak locations and increased peak intensity after HCl-purification supports the conclusion, which states that the purification process substantially lowered the impurity content of natural indigo pigment without altering or degrading its chemical structure. The ATR-FTIR data of the pigment powders are presented in Figure 3.

In **Publications I**, **II**, and **III**, all biocolorants were applied as dried powders. An image processing software was used to approximate median particle size of the colorant powders based on high-resolution images acquired from an optical microscope. Based on the image processing analysis, all colorant powders presented median particle diameters ranging from 3 µm to 8 µm. Visually, both indigo pigments had a deep blue color, the madder extract was dark red, and the weld extract showed an intense yellow color with brownish tint. In contrast to the high-chroma colorants obtained from the dried plant extracts, the colors of the black biochar colorant and the brown kraft lignin colorant were substantially more desaturated, low-chroma tones.

4.2 Wood coatings

In **Publication I**, linseed-oil based paint and varnish bases for wood coating applications were pigmented using an unpurified natural indigo pigment extracted from *Isatis tinctoria* leaves. Furthermore, color stability of the biocolored coatings was determined using an accelerated weathering test. Finally, the stability properties of the biocolored coatings were compared to uncolored coatings and reference coatings colored with synthetic indigo pigment and a commercial ultramarine pigment. Figure 4 shows the visual appearance of wooden panels coated with different coating formulations before and after 40 days of artificial weathering.

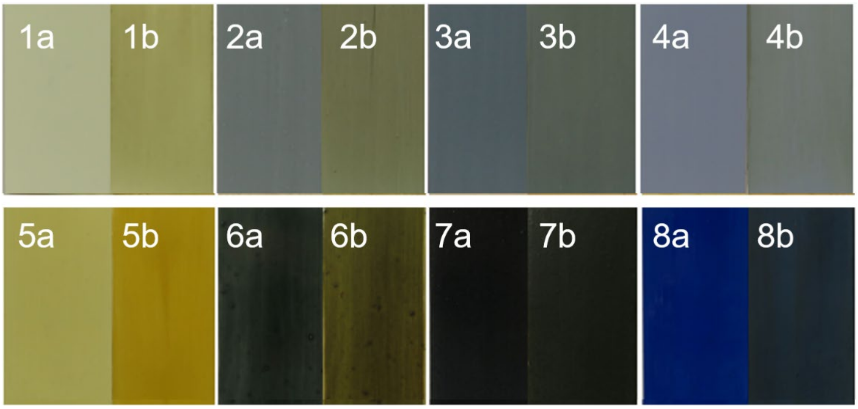

Figure 4. Photographs of the painted (**1** – **4**) and varnished (**5** – **8**) specimens before and after the 40 days exposure testing. Pigments of specimen pairs from left to right: unpigmented (**1** and **5**), natural indigo (**2** and **6**), synthetic indigo (**3** and **7**) and ultramarine pigment (**4** and **8**). The unexposed specimens are labeled with **"a"** and exposed specimens with **"b"**. Reproduced from **Publication I** with permission from Wiley-Blackwell.

Colorimetric inspection of the coatings during the weathering period showed that the slightly greenish yellow colors of the unpigmented paint and varnish coatings substantially shifted towards redder hues. This hue change was especially prominent in the unpigmented varnish, which also presented a drastic increase in chromaticity over time. Moreover, lightness values of both unpigmented coatings substantially decreased during weathering. In contrast, the pigmented coatings presented only minor changes in lightness during weathering. However, due to the yellow initial color of the unpigmented coatings, the coatings containing either natural or synthetic indigo presented greenish initial colors instead of the deep blue appearance characteristic to indigo pigments. Furthermore, the initial pure green hues of indigo-pigmented coatings gradually changed towards more yellow and even slightly red shades during the weathering exposure. On the other hand, both coatings with commercial ultramarine pigment presented an intense blue initial color, which exhibited a substantial shift towards green hues during the weathering period. Colorimetric values of all coated specimens are shown in Figure 5.

Notably, the coatings pigmented with indigo pigments presented substantially lower total color changes compared to the unpigmented and commercially pigmented coatings. As indigo pigments are known to possess a high absorbance and stability towards UV light, it is likely that the indigo pigments slowed down the color changes caused by coating degradation during weathering.[103, 241] Nevertheless, both coatings pigmented with synthetic indigo showed less changes in colorimetric values over time compared to the coatings colored with natural indigo pigment. The superior stability performance achieved with the synthetic pigment was likely due to its higher purity, as explained in the previous subchapter.

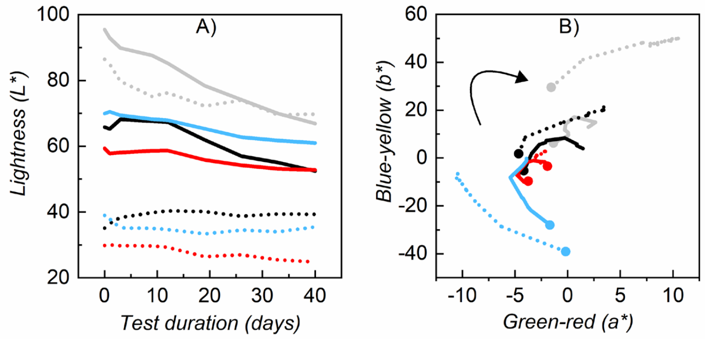

Figure 5. Development of **A)** CIE L^* and **B)** CIE a^* and b^* colorimetric values during the exposure period. The solid lines represent painted specimens, and dotted lines represent varnished specimens. Color coding of the pigments: black = natural indigo, red = synthetic indigo, blue = ultramarine pigment and gray = uncolored coating. Reproduced from **Publication I** with permission from Wiley-Blackwell.

In addition to colorimetric analysis, stability of the pigments and coating matrices were investigated by also analyzing reflectance spectra of the coated specimens. As presented in Figure 6, reflectance spectra of the colored coatings in the visible 360–700 nm wavelength range showed initial peak maxima in the 430–470 nm region, which is characteristic to blue pigments. During the weathering period, changes in maximum reflectance peak location were observed especially in the varnished specimens, which all experienced gradual shift of the maximum reflectance peak towards higher wavelengths. Thus, the peak shift from blue 430–470 nm wavelength region towards green and yellow regions was likely due to ageing behavior of the unpigmented varnish, which led to visible yellowing of all varnished specimens. Even though the peak shifting phenomenon was more pronounced in the indigo-pigmented varnishes, the unpigmented and ultramarine-pigmented varnishes showed substantially larger decrease in relative reflectance at 430 nm over exposure time. Thus, due to different patterns of spectral development observed in each varnish, little conclusions could be made about pigment degradation inside the varnish matrices based on the spectral ageing alone.

For the paint coatings, on the other hand, a substantial peak shift was only detected for the indigo-colored coatings, but not for the uncolored and ultramarine-colored paints. The peak shift in indigo-colored paints may suggest photo-oxidative degradation of indigo pigments during weathering, potentially catalyzed by the presence of titanium dioxide pigment in the base paint. Although titanium dioxide is effective in formulating fully opaque paint coatings, a previous study has shown that it may substantially accelerate photodegradation of solid indigo pigment.[242] Notably, the light source in the weathering equipment radiated in UV-A wavelength region, which overlaps with absorption bands of both indigo and titanium dioxide pigments. However, no traces of photoreaction products of indigo could be detected in the ATR-FTIR analysis due to complex chemical compositions of the coating matrices. Spectral evolution of the coatings during the exposure period is presented in Figure 6.

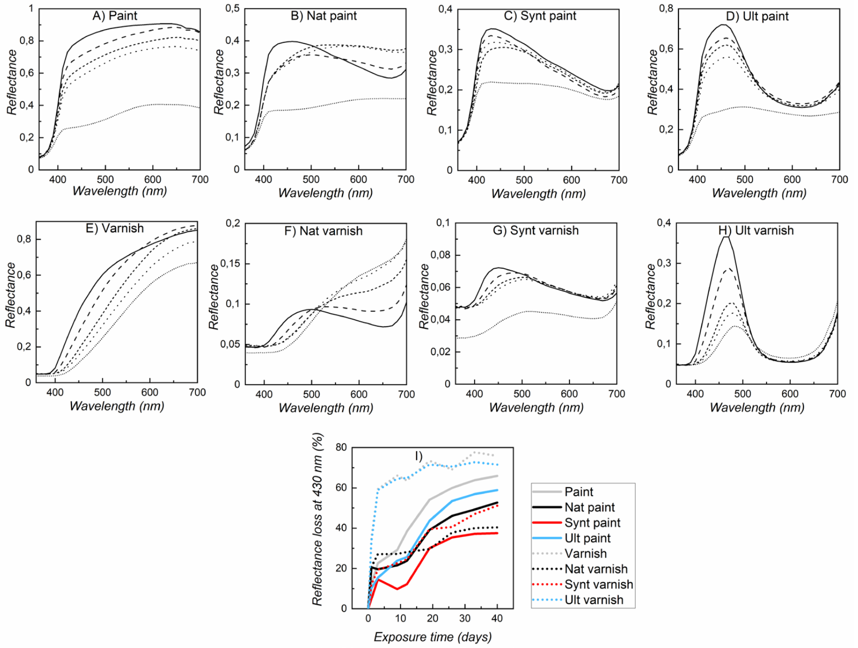

Figure 6. Development of visible reflectance spectrum of the samples during the exposure period (subfigures **A – H**) and reflectance and reflectance loss at 430 nm over exposure time (subfigure **I**). In subfigures **A – H**, spectra were measured before exposure (solid line) and after 1 day (long dashed line), 3 days (dashed line), 9 days (dotted line) and 40 days (small, dotted line) of exposure. Reproduced from **Publication I** with permission from Wiley-Blackwell.

Degradation of the coating matrices was investigated by measuring reflectance peak intensity, hyperspectral reflectance, and ATR-FTIR spectra of the coated specimens before and after the accelerated weathering. Hyperspectral reflectance of the paint coatings in 700–1000 nm wavelength range presented a drastic decrease in intensity after the weathering period. In contrast, substantially lesser decreases in reflectance were observed in the varnish matrices, even though both coating types initially presented similar reflectance properties in the hyperspectral region. The difference in reflective properties between paint and varnish matrices indicates that the paints were highly sensitive to the degradative effects of weathering, whereas the varnishes showed substantially higher degradation resistance. Regarding the degradation of the varnish matrices, the varnishes colored with indigo pigments showed more minor changes in hyperspectral reflectance compared to the unpigmented and commercially pigmented varnishes. This indicates higher degradation resistance in the varnishes pigmented with the indigo pigments, which is further supported by the substantially lower relative reflectance losses observed in the visual wavelength region. Hyperspectral reflectance of the coatings before and after 40 days of artificial weathering is presented in Figure 7.

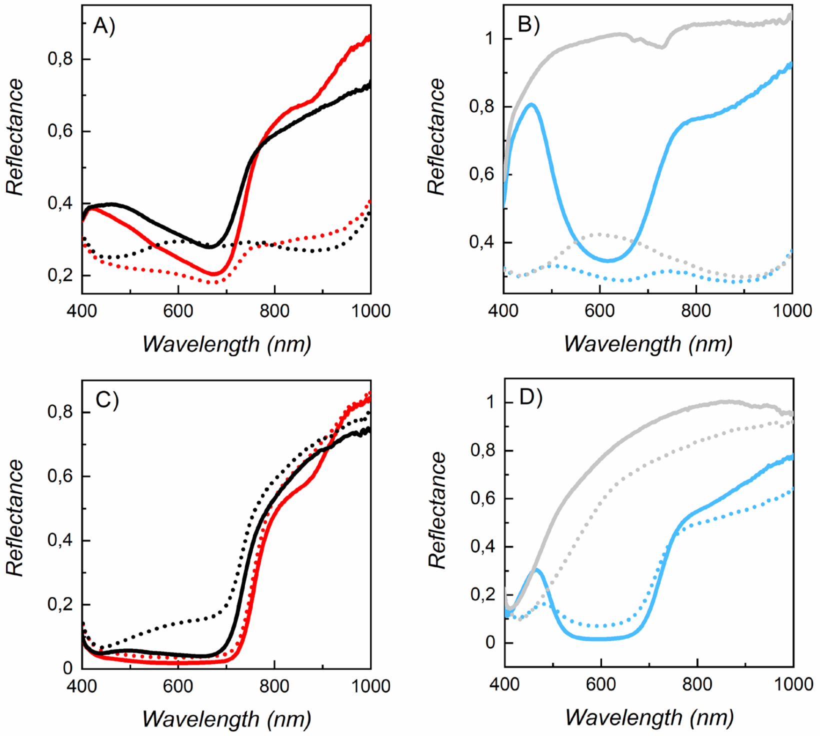

Figure 7. Hyperspectral reflectance of the coated specimens before and after the 40 days of artificial weathering. Painted specimens are presented in subfigures **A)** and **B)**, and varnished specimens are presented on subfigures **C)** and **D)**. Unexposed specimens are presented with solid lines and exposed specimens with dotted lines. Color coding of the pigments: black = natural indigo, red = synthetic indigo, blue = commercial pigment and gray = no pigment. Reproduced from **Publication I** with permission from Wiley-Blackwell.

As seen from the ATR-FTIR spectra in Figure 8, all unexposed coatings presented a –C–C peak at 2923 cm^{-1}, a –C=C peak at 2853 cm^{-1}, and a strong –C=O ester peak at 1740 cm^{-1}, which are all typical to linseed oil-based coatings.[243] Furthermore, all specimens showed a peak at 1166 cm^{-1}, which corresponds to ester linkages in the linseed oil structure.[244] The characteristic peaks for different pigments were relatively minor in the unexposed coatings, although distinctive bands at 1615 cm^{-1} for the indigo-colored coatings and at 980 cm^{-1} for the ultramarine-colored coatings could be detected. Additionally, all paint coatings presented heightened absorption in the 550–750 cm^{-1} area, presumably representing the Ti–O–Ti and Ti–O bonds in the titanium dioxide base pigment.[245] Thus, in the aged specimens, substantial spectral overlap between pigments and the binder was present in the wavenumbers lower than 1650 cm^{-1}. The main IR peaks of unexposed varnish coating are listed in Table 2.

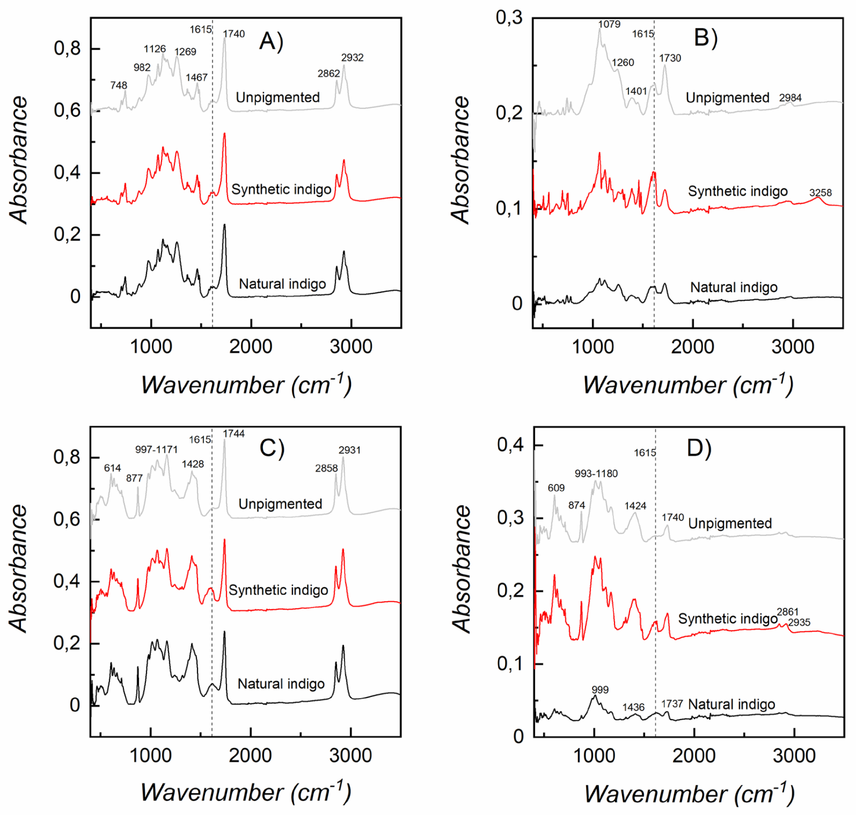

Figure 8. ATR-FTIR spectra of the coated wooden specimens. **A)** varnished specimens before weathering, **B)** varnished specimens after weathering, **C)** painted specimens before weathering, and **D)** painted specimens after weathering. Reproduced from **Publication I** with permission from Wiley-Blackwell.

Despite the potential spectral interference between pigments and linseed oil binders in the lower wavenumbers, binder degradation in the aged specimens was clearly indicated by substantial changes in the –C=O stretching peak. After the weathering period, location of the –C=O stretching peak had shifted from 1737 cm^{-1} to 1719 cm^{-1} in the varnish coatings and from 1740 cm^{-1} to 1732 cm^{-1} in the paint coatings. The –C=O peak shift towards lower wavelengths indicates decreased concentration of the ester bonds and simultaneous increase in carboxylic acids, which in turn suggests breaking of the ester linkages into –COOH and –OH end groups.[244, 246] Furthermore, broadening of the –C=O stretching peak and a shoulder formation in the 1760–1800 cm^{-1} range indicate degradation of a linseed oil binder into fatty acids by simultaneous hydrolysis and photolysis reactions.[247] Only minor differences in IR spectra between the different pigments were observed in both coating types, for instance, the pigments had seemingly no effect on magnitude of the carbonyl peak shift and peak proportions of the aged coatings. Although the differences were small, in the paint coatings, the emergence of a peak shoulder at 1770 cm^{-1} was most prominent in the ultramarine coating, and most notable shoulder at 1710 cm^{-1} was observed in the natural indigo and ultramarine coatings. Regarding the varnishes, the largest increase of intensity at 1770 cm^{-1} appeared in the unpigmented coatings and at 1710 cm^{-1} in the natural indigo coating.

Table 2. Main IR peak locations of the linseed-oil based varnish coatings pigmented with natural indigo.

Functional group	Wavenumber (cm^{-1})
C–C	2923
C=C	2853
C=O (esters in the linseed oil)	1740
C=O (ketones in the indigo)	1615
C–H	1467
C–O (esters in the linseed oil)	1166

In conclusion, even though only minor differences between pigments were observed, the most stable behavior was achieved with the synthetic indigo pigment in both coating matrices. Furthermore, the natural indigo pigment did not conclusively improve chemical stability of the linseed oil binders during weathering despite offering protection against reflectance changes in the varnish coatings. Nevertheless, both indigo pigments retained their most characteristic IR band at 1615 cm^{-1} in both coating matrices during weathering, which indicates at least some degree of pigment stability even in the paint coatings with titanium dioxide.

4.3 Polypropylene for additive manufacturing

In **Publication II**, a mixture of virgin PP powder and HCl-purified natural indigo pigment was used to manufacture biocolored specimen rods via filament extrusion and additive manufacturing. Notably, biocolored specimens containing unpurified natural indigo pigment and synthetic indigo pigment were manufactured in the same manner. None of the indigo colorants, up to the studied additive concentration of 0.5 w-%, substantially affected the filament extrusion or additive manufacturing processes compared to uncolored PP; on the contrary, all plastics exhibited identical behavior during thermal processing. Moreover, visual inspection after additive manufacturing of the indigo-colored specimen rods showed that all samples had an even color with no visually distinguishable colorant particles. Thus, the preliminary conclusion was that the indigo colorants in this study could have potential to be utilized as coloring agents for thermally treated PP matrices. Photographs of the specimen rods are presented in Figure 9.

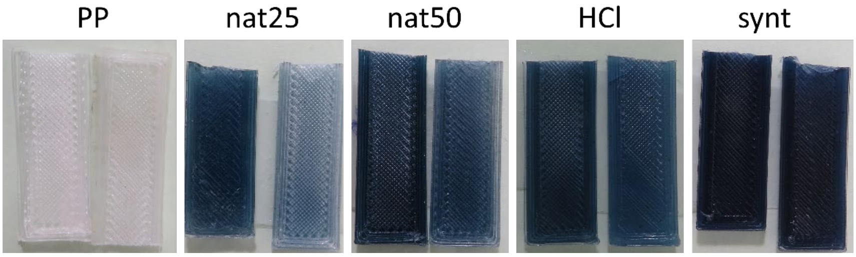

Figure 9. Pieces of the 3D-printed polypropylene specimens before and after Xenon light exposure. The unexposed specimens are on the left side and their exposed counterparts are on the right side. Specimen coding: **PP** = no pigment, **nat25** = 0.25 w-% natural indigo, **nat50** = 0.50 w-% natural indigo, **HCl** = 0.25 w-% purified natural indigo, and **synt** = 0.25 w-% synthetic indigo. Reproduced from **Publication II** with permission from Emerald Publishing Group.

Color-wise, in both visual and colorimetric inspection, all indigo-colored specimens exhibited a distinctive and deep indigo-blue color. Notably, the specimen rods containing 0.25 % of HCl-purified pigment exhibited stronger color compared to the specimens colored with 0.25 % of unpurified pigment. However, an equally strong color was achieved by increasing concentration of the unpurified pigment to 0.50 %. Nonetheless, the strongest color was achieved with the synthetic indigo pigment, which also presented a slightly reddish hue according to the colorimetric values. In contrast, a minor green tint was detected in the natural indigo specimens. However, despite being significant in colorimetric presentation, the hue differences were indistinguishable by visual inspection. Finally, the unpigmented specimen was highly transparent and almost colorless, which is typical for PP.[248]

Lightfastness of the pigmented specimens was determined under continuous Xenon light exposure, which decreased the *K/S* color intensity of all pigmented specimens. As expected, no colorimetric changes were observed in the unpigmented specimen, which highlights the remarkably high photostability properties of virgin PP. The most substantial changes were observed in the specimens with 0.25 % of unpurified natural indigo, which showed the highest relative loss in *K/S* value among the colored specimens. Furthermore, the specimens with 0.25 % of unpurified pigment showed the highest average differences in lightness, reflectance, and total color. Unsurprisingly, the most stable color was observed in the synthetic indigo specimens, which only showed a minor drop in color intensity after 168 hours of exposure. Interestingly, the specimens containing 0.25 % of HCl-purified indigo and the specimens with 0.50 % of unpurified natural indigo exhibited almost identical development in *K/S* values, lightness and total color during the exposure. Both specimen types went through significantly less changes in color intensity compared to the specimen with 0.25 % of unpurified pigment but changed substantially more than the synthetic indigo specimen.

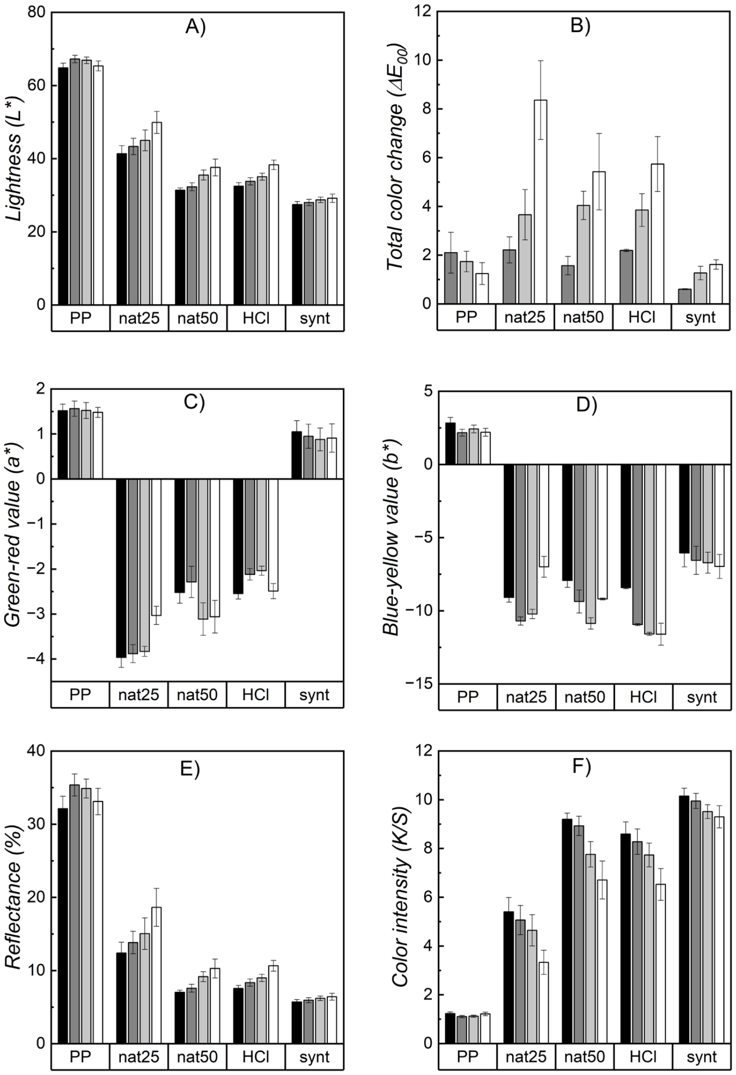

Figure 10. Colorimetric values of the 3D-printed polypropylene specimens before and after 24, 72, and 168 hours of Xenon light exposure. Color parameters in the subfigures: **A)** Lightness L^*, **B)** Total color change ΔE_{00}, **C)** Green-red value a^*, **D)** Blue-yellow value b^*, **E)** Reflectance, **F)** Color intensity K/S. Exposure times by bar color: black = 0 h, gray = 24 h, light gray = 72 h, and white = 168 h. Specimen coding: **PP** = no pigment, **nat25** = 0.25 w-% natural indigo, **nat50** = 0.50 w-% natural indigo, **HCl** = 0.25 w-% purified natural indigo, and **synt** = 0.25 w-% synthetic indigo. Reproduced from **Publication II** with permission from Emerald Publishing Group.

Regarding color characteristics, the specimens with 0.25 % of unpurified pigment showed a statistically significant decrease of blue color parameter after 168 hours of exposure. The loss of blue color was not observed in the other specimens; in contrast, all other pigmented specimen types experienced minor shift towards even more intense blue color. Moreover, the specimen with 0.25 % of unpurified pigment exhibited a substantial green-to-red color shift, which was not observed in any other specimen type. Again, the other natural indigo pigmented specimens presented almost identical colorimetric changes, which were minor compared to the specimens with 0.25 % of unpurified pigment but more substantial than those observed with the specimens pigmented with synthetic indigo. Thus, the HCl-purification substantially increased lightfastness and color stability provided by the natural indigo pigment, when both pigments are used in equal concentrations. Colorimetric evaluation of all specimens before and after the Xenon light exposure is presented in Figure 10.

ATR-FTIR analysis of all PP specimens showed the characteristic CH_3 bands at 1376 cm^{-1}, 1458 cm^{-1}, and at 2840–2960 cm^{-1} wavenumber range.[249] In ATR-FTIR analysis, formation of carbonyl groups during oxidative degradation of PP can regularly be detected as peak growth in the 1580–1830 cm^{-1} wavenumber range.[250] Furthermore, photo-oxidative degradation would also cause emergence of broad band around 2840–2960 cm^{-1} due to hydroxyl groups in the oxidation products.[251] However, emergence of neither carbonyl nor hydroxyl peaks could be observed in the IR spectra after Xenon light exposure, which suggests high photostability for all specimens. In conclusion, based on the colorimetric and spectral observations, the light exposure affected the pigments inside PP matrix but not the plastic matrix itself. As it stands, none of the indigo pigments supplemented the plastic with photo-protective properties but did not accelerate its photodegradation either. Even though the best color fastness was achieved with the synthetic indigo pigment, the HCl-purified natural indigo pigment presented a substantial improvement over the unpurified pigment. However, increasing the amount of unpurified pigment inside the PP matrix from 0.25 w-% to 0.50 w-% improved its lightfastness performance to similar levels with the matrix colored using HCl-purified pigment. Thus, it remains uncertain whether the photostability differences between the PP specimens originated from the different impurity content, pigment content, or both characteristics of the pigment powders simultaneously.

4.4 Polylactic acid for injection molding

In Publication III, biocolored specimen rods suited for tensile testing were injection molded from an extruded mixture of virgin PLA granules and biocolorant powders. Visual inspection of the biocolored specimens showed that lignin, dried weld extract, and dried madder extract all produced evenly colored PLA specimens with no visible colorant particles. In contrast, the biochar and indigo-colored specimens both contained visible colorant particles inside the plastic matrix. However, the colorant particles in biochar-colored specimens were evenly distributed and barely distinguishable, giving an illusion of an even and opaque black color for a human observer in regular illumination. Thus, clear agglomeration of pigment particles was only observed in the indigo-colored specimens. Despite the formation of pigment agglomerates during thermal processing, the indigo-colored PLA specimens presented a highly distinctive blue color. In addition to visual inspection, image processing analysis of photos acquired using optical microscope showed that all colored specimens had approximate median particle sizes of 3–8 μm. Furthermore, SEM images of the specimens showed no signs of surface deformations or substantial differences between different specimens. Visual photographs and SEM images of the specimens are presented in Figure 11.

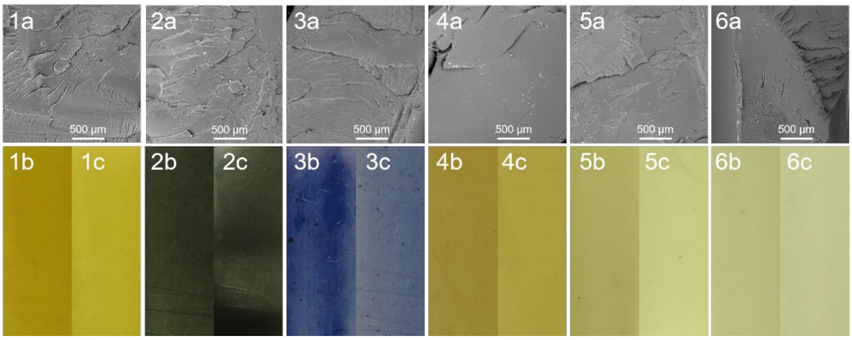

Figure 11. Images of the injection molded PLA rods. Top row **(a)**: SEM images with 100x magnification. Bottom row: Photographs before **(b)** and after 168h **(c)** of Xenon light exposure. Colorants: **1)** madder extract, **2)** biochar, **3)** indigo, **4)** lignin, **5)** weld extract and **6)** no colorant. Reproduced from **Publication III** with permission from Wiley-Blackwell.

Lightfastness performance of the biocolored PLA specimens were determined by exposing the specimens to continuous radiation from a Xenon arc light source. As presented in Figure 12D, visual lightfastness evaluation of the specimens before and after the 168-hour exposure period showed that biochar-colored and lignin-colored specimens both had good lightfastness ratings comparable to the uncolored reference specimen. The specimens colored with dried madder and weld extracts presented substantially lower, but nevertheless intermediate lightfastness ratings, whereas the indigo-colored specimen achieved a slightly weaker rating compared to the two plant extracts. Even though none of the specimens presented a poor lightfastness rating, the medium-to-low lightfastness performance of natural indigo was particularly unexpected due to generally high stability of indigo pigments. Likely, the low lightfastness of indigo pigment is partially explained by the pigment agglomeration phenomenon, which decreased the concentration of evenly distributed pigment outside the agglomerates. Although a certain degree of pigment agglomeration generally leads to improved lightfastness, in this case the agglomerates were too large to contribute to the overall color impression of the polymer. Hence, the pigment agglomeration merely decreased the concentration of evenly distributed pigment outside the agglomerates, leading to lowered lightfastness in evenly colored parts of the polymer.[73]

Reinforcing the observations from visual inspection, colorimetric analysis of the biocolored PLA specimens shown in Figures 12A-C presented only minimal color changes in the biochar-colored specimen after the exposure period. Furthermore, similar to the visual inspection, the colorimetric evaluation showed largest color changes in the indigo-colored specimens, which experienced substantial increase in CIE parameters L^* and b^*, indicating increased lightness and yellowness. Additionally, substantial decreases in contrast ratio (*CR*) and CIE color parameter a^* were observed in the indigo-colored PLA, showing increased transparency and greenness during ageing.

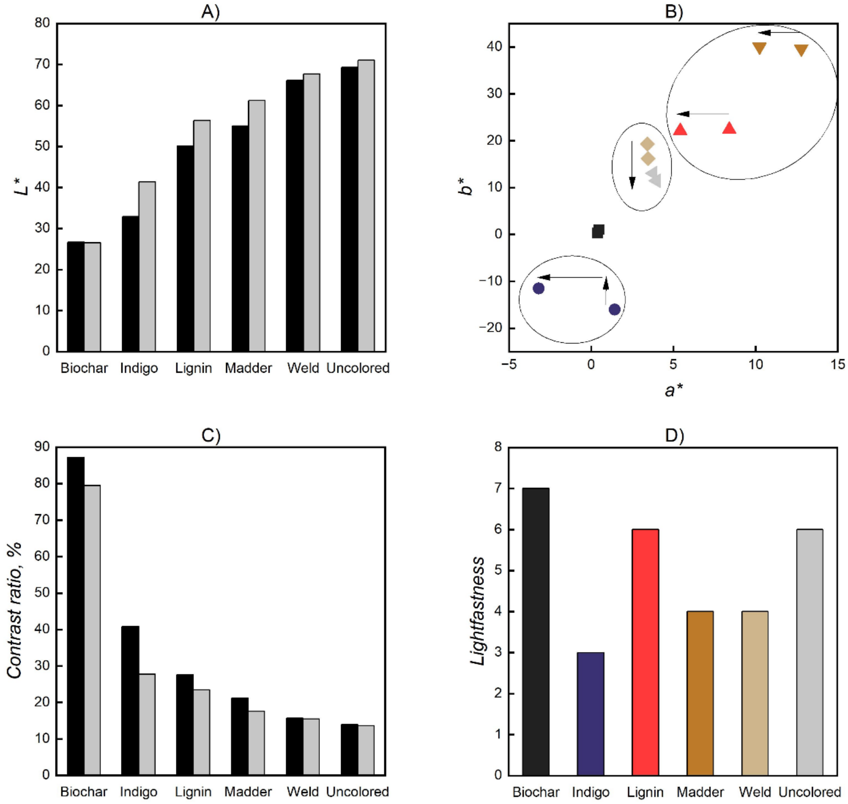

Figure 12. **A)** Colorimetric CIE L^* values, **B)** colorimetric CIE a^* and b^* values, and **C)** contrast ratios of the biocolored PLA rods before and after the exposure period. **D)** Lightfastness ratings of the biocolored PLA rods. In subfigures A and C, black bars represent unexposed specimens, and gray bars represent exposed specimens. Reproduced from **Publication III** with permission from Wiley-Blackwell.

In contrast to biochar and indigo, colorimetric evaluation of the lignin- and madder-colored specimens did not completely support the observations from visual lightfastness evaluation. Although a clear distinction on lightfastness performance between the lignin- and the madder-colored specimens was seen in visual observation, both specimens showed similar levels of increase in colorimetric L^* value and decreases in *CR*, and a^* values. These color changes were not observed in the uncolored PLA, which suggests photodegradation of the lignin and madder extract colorants. This type of light-induced degradation is characteristic to polyphenolic compounds, such as kraft lignin and madder extract, due to their high light absorbance in ultraviolet wavelengths.[112, 252, 253] Nevertheless, controlled photodegradation of a polyphenolic additive may reduce degradation in the polymer matrix.[254, 255] However, despite the polyphenolic nature of weld extract colorant, stable colorimetric behavior was observed in the weld-colored specimen, which only experienced a minimal loss in yellowness during the exposure. Nonetheless, due to the minimal differences in initial color between the weld-colored and uncolored specimens, major color changes would have been highly unexpected due to high color stability of the uncolored PLA.

Even though visual and colorimetric inspection showed substantial differences in lightfastness performance between different colorants, none of the specimens presented major changes in their reflective properties. Investigation of reflectance spectra of the PLA specimens in 400–700 nm and 800–1000 nm wavelength regions showed no significant changes in either peak location or peak intensity during the exposure period. Thus, despite the distinguishable differences in lightfastness performance between the biocolorant additives, all specimens proved to be relatively resistant to photodegradation.

Possible chemical alterations in the polymer matrix during the Xenon light exposure were investigated with ATR-FTIR analysis. As presented in Figure 13A, the IR spectra in 4000–400 cm^{-1} wavenumber range showed an identical composition of absorbance peaks for all PLA specimens irrespective of biocolorant additive or degree of Xenon light exposure. The presence of –C–O bonds characteristic to the ester groups in virgin PLA was indicated by the vibrating stretch peaks at 1081, 1130, and 1181 cm^{-1}, and the corresponding –C=O carbonyl end groups were indicated by a strong stretch peak at 1747 cm^{-1}. Moreover, presence of the stable $-CH_3$ groups could be observed as a bending peak at 1453 cm^{-1} and the –CH– groups as a pair of bending peaks located at 1362 cm^{-1} and 1382 cm^{-1}. In addition, mostly amorphous structure of the polymer matrix was indicated by the 957 cm^{-1} peak and the absence of a peak at 921 cm^{-1}, which would indicate presence of crystalline PLA structures.[256–258]

Even though emergence of new shoulder bands related to the existing IR peaks was not detected after Xenon light excitation, proportional intensity of the peaks changed substantially during the exposure period. Relative to the photo-stable $-CH_3$ peak at 1453 cm^{-1}, the carbonyl peak at 1747 cm^{-1} showed a substantial increase in intensity for most specimens after the exposure period. Previous studies have shown that increased concentrations of –C=O groups during intense light exposure may indicate photodegradation by Norrish Type II reaction, which breaks the ester bonds of PLA into –COOH and –OH end groups.[259–261] However, the substantial carbonyl peak growth may also result from different photodegradation mechanism, where diketone end groups are formed instead.[262, 263] Nevertheless, appearance of neither anhydride band at 1845 cm^{-1} nor carboxylic acid band at 1720 cm^{-1} was observed in the IR spectra of exposed specimens, which would be characteristic for both photodegradation reactions.

Due to absence of both anhydride and carboxylic acid bands in the exposed specimens, numerical changes in carbonyl index values presented in Figure 13B were calculated to quantify the degree of polymer degradation in each specimen. Carbonyl index is a numerical value calculated by dividing carbonyl peak intensity by the stable $-CH_3$ peak intensity, and the change of carbonyl index during exposure has been utilized in multiple previous studies to estimate degree of PLA photodegradation.[264–266] Expectedly, the highest change in carbonyl index was determined for the uncolored specimen due to absence of protective pigment additives. Compared to the unpigmented specimen, substantially lower changes in carbonyl index were observed in the colored specimens. The significantly higher change in carbonyl index value suggests that all pigments in this study offered substantial photoprotection for the polymer matrix. Notably, the change in carbonyl index value was close to zero in the lignin-colored specimen, which indicates that the lignin biocolorant offered almost complete photoprotection for the polymer matrix under Xenon light exposure. The substantial photoprotective ability of kraft lignin was presumably caused by large amount of UV-absorptive functional groups in the lignin structure. The UV-absorptive groups probably absorbed most of the damaging short-wavelength fraction of the Xenon light, which substantially decreased the photo-oxidative radiation load directed on the polymer matrix.

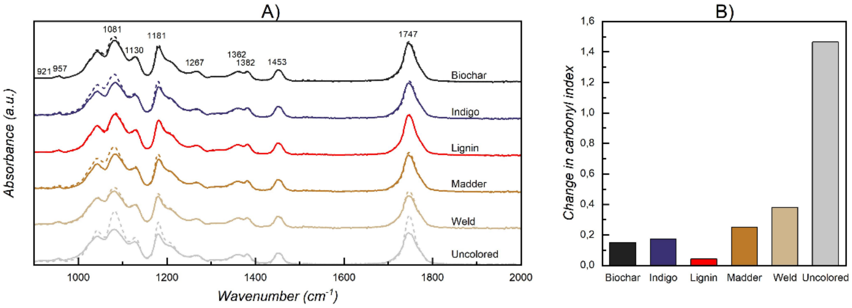

Figure 13. A) ATR-FTIR spectra of biocolored PLA specimens before (solid line) and after 168 h (dashed line) of Xenon light exposure. **B)** Increase in carbonyl indices of the biocolored PLA specimens after 168 h of Xenon light exposure. Reproduced from **Publication III** with permission from Wiley-Blackwell.

Mechanical performance of all unexposed specimens was determined by tensile test to detect possible negative effects of the biocolorant additives to strength of PLA. The tensile test data for each specimen showed no significant differences in elongation properties. However, as presented in Figure 14, statistically significant differences between specimen types were observed in both ultimate tensile strength values and Young's moduli. Surprisingly, compared to uncolored PLA, the lignin-colored polymer presented significant improvement in both ultimate tensile strength and Young's modulus. Due to the relatively low biocolorant concentration in the specimens, positive effects to mechanical properties were rather unexpected. Nonetheless, the improved strength properties probably resulted from interfacial interaction between PLA and lignin, where the kraft lignin particles reinforce the polymer matrix by evenly distributing the mechanical loads. Thus, a higher external force is required to create high enough local loads to induce local void formation, which would eventually lead to polymer crazing followed by crack formation and mechanical failure under continuous tensile stress.[267]

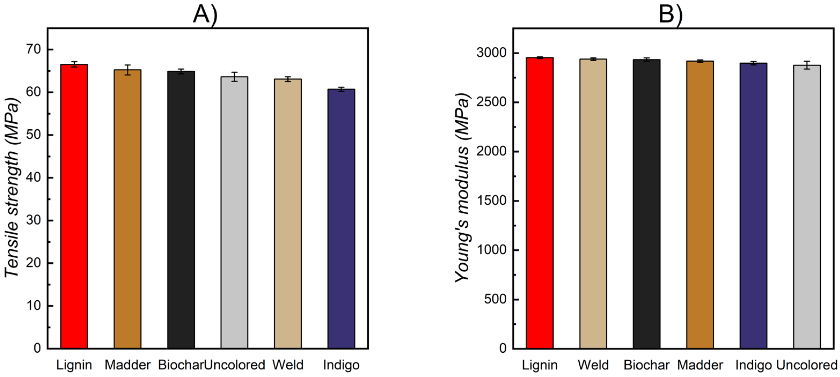

Figure 14. A) Tensile strength and **B)** Young's modulus of the biocolored PLA specimens. The error bars represent 95 % statistical confidence interval based on eight parallel tensile tests. Reproduced from **Publication III** with permission from Wiley-Blackwell.

Although the interfacial behavior of PLA-lignin composites is by no means a novelty in scientific literature, most studies have been conducted with substantially higher lignin concentrations.[268] As presented in this thesis, similar effects can be achieved with colorant-level concentrations as well. Besides lignin, lesser but statistically significant improvements in tensile strength were also achieved with madder extract and biochar pigments. On the other hand, a significant negative effect for tensile properties was observed in the indigo-colored polymer. Although no difference in Young's modulus was observed, the indigo-colored polymer presented substantially lower ultimate tensile strength compared to uncolored PLA, presumably due to the presence of pigment agglomerates inside the polymer matrix.

4.5 Anodized aluminum

A series of unpublished trials were conducted to investigate potential of madder extract and weld extract biocolorants for dyeing of anodized aluminum surface. Visual and microscopic examinations showed that the combination of anodization, dyeing, and sealing processes produced a hard colored aluminum oxide layer on the surfaces of the aluminum specimens. SEM images of the anodized and dyed porous aluminum oxide layers shown in Figure 15 present approximately equal pore distribution and pore size in the aluminum oxide layers irrespective of colorants used. Notably, agglomerations or deformations of neither dye could be detected from the images, which indicates that the dye molecules were evenly trapped inside the sealed pores.

As presented by the visual photographs in Figure 15, an evenly colored aluminum oxide layer with strong, metallic color was achieved with both biocolorants in acidic dyeing conditions. In addition to visual inspection, the high level of integrity of the colored layer was verified by examination with optical microscope, which showed no defects or colorless areas on the aluminum oxide surface. In colorimetric inspection, the specimens dyed with weld extract in pH 5.0 dyebath presented intense yellow colors with moderate greenish hue. Moreover, a comparable but slightly less intense color was achieved with the weld extract in pH 6.5 dyebath as well, however, increasing the dyebath pH to 8.5 resulted in significantly weaker color compared to the other two specimens. Similar pH-dependency in color was observed on surfaces dyed with madder extract. The specimen dyed with madder extract in pH 5.0 dyebath had an even more intense color than the corresponding weld-colored specimen, and it presented a red shade characteristic to madder-based dyes. However, as observed in the weld-colored specimens, increasing the pH to 6.5 resulted to slight decrease in color strength and only a weak color was achieved when the dyeing was conducted in pH 8.5 dyebath.

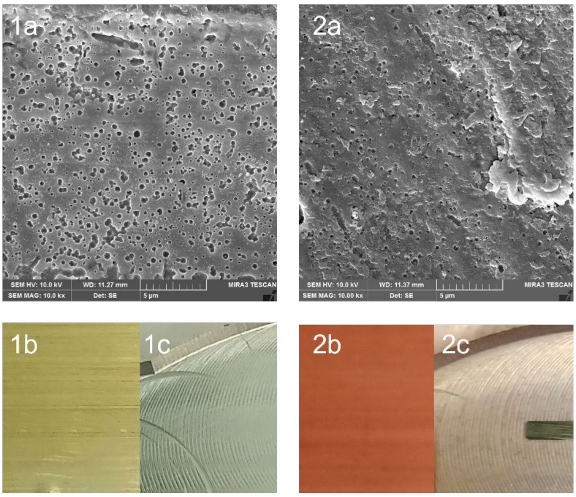

Figure 15. Images of biocolored anodized aluminum. Top row **(a)**: SEM images with 10000x magnification. Bottom row: Photographs before **(b)** and after 24 h **(c)** of Xenon light exposure. Colorants: **1)** weld extract, and **2)** madder extract.

Lightfastness of the dyed surfaces was determined by exposing the colored specimens to controlled radiation from a Xenon light source. After the exposure period, substantial decrease in color intensity and almost total loss of color was observed in all weld-colored specimens. Despite being slightly less susceptible towards color changes, the specimens dyed with madder extract exhibited substantial loss in color and intensity as well. Furthermore, even though the initial color intensity was higher in the specimens dyed in pH 5.0 for both colorant types, higher acidity of the dyebath did not substantially increase photodegradation resistance of the dyes in the anodized surface. As discussed previously in conjunction with PLA specimens, some degree of photodegradation is typical for polyphenolic colorant substances, such as alizarin in madder extract and luteolin in weld extract. Nevertheless, low photostability of madder and weld biocolorants was expected, given that most organic dyes exhibit low photostability in anodized coatings due to low dye concentration and high specific surface area of the porous oxide layer.[269, 270] Only few studies concerning lightfastness of organic pigments in anodized coatings have been conducted, and most of them suggest application of various pore sealing techniques to improve lightfastness of organic anodizing dyes.[271] However, the mechanisms contributing to rapid photodegradation of organic dyes inside the porous layer remain quite unexplored.

5. Conclusions

This thesis investigated multiple potential applications for biocolorants in engineering materials. The results showed that even and intense coloration can be readily achieved with biocolorants, whether applied to wood coatings, thermoplastic polymers, or anodized surfaces. The general ease of substituting a commonly used colorant with a bio-based one was particularly well illustrated in **Publication I**, in which no additional preparation was required to tint varnish coatings with natural indigo pigment instead of a conventional ultramarine pigment. Moreover, compared to ultramarine-pigmented coatings, higher relative color stability was seen in the varnishes pigmented with natural indigo. Even though the observed stability differences between natural indigo and commercial ultramarine pigment were not large, the experiments with wood coatings neatly showcased how a dried biocolorant powder can occasionally outperform even regularly used commercial pigments despite containing some impurities.

In addition to merely offering a bio-based substitute to inorganic or synthetic colorants, biocolorants can provide additional value by improving photodegradation resistance or even strength properties of the colored matrix, which was especially highlighted by the results in **Publication III**. Despite the relatively low colorant concentration, significant improvements to durability properties of PLA were achieved with multiple biocolorants. Very promising results were achieved with kraft lignin, in particular, which offered the PLA matrix almost full photodegradation resistance and significantly higher tensile strength compared to other studied colorants. Going forward, the added functional value from biocolorants offers a particularly strong motivation to continue exploring bio-based coloring solutions not only for textiles, but for engineering materials as well.

Even though biocolorants may improve functionality and sustainability of engineering materials in many cases, this thesis has also shown that for certain biocolorants, low lightfastness and variance in purity may pose technical challenges. The case of low lightfastness was especially highlighted in **Chapter 4.5** of this thesis, which showed how even relatively short period of Xenon light exposure may lead to substantial dye degradation in biocolored aluminum oxide layers. Although less drastic biocolorant photodegradation was observed with natural indigo pigment in **Publications I** and **II**, both publications showed that systematically higher lightfastness properties could be achieved with synthetic indigo pigment irrespective of application. To a certain extent, these lightfastness challenges observed with bio-based indigo were explained by its substantial impurity content as characterized in **Publication II**. Nevertheless, as also seen in **Publication II**, substantial improvements on coloration properties and lightfastness stability of the natural pigment can be achieved even with a rudimentary HCl-purification process. However, even after purification, the natural pigment was still inferior to its synthetic counterpart in terms of purity, color intensity, and lightfastness. In addition to potential impurities, such as metallic oxides, the presence of photocatalytic compounds in the biocolored matrices may accelerate photodegradation of an organic biocolorant. An instructive example of accelerated photodegradation was seen in **Publication I**, where degradation of natural indigo pigment in a paint coating was accelerated by titanium dioxide base pigment.

As an important note, analyzing ecological impact, toxicology, and financial viability of biocolored materials is mostly beyond the scope of this thesis. Nevertheless, careful study of these aspects is absolutely essential to materialize the perceived sustainability status of biocolorants and to ultimately transform academic research into practical applications. As discussed briefly in both **Chapter 2.4** and **Publication III**, certain low-value industrial side streams could create optimal feedstocks for biocolorant production to maximize raw material availability, cost effectiveness, and ultimately the sustainability impact of biocolorant use. Such waste-to-valuable biocolorants may include, for instance, onion peel extracts, bark extracts, and the kraft lignin familiar from this thesis. Nevertheless, neither agricultural nor microbial pathways for biocolorant production should be disregarded, as they present opportunities to produce a broader variety of colorants especially suited for specific eco-luxury applications. Even though many of the high-value biocolorants would only be used in small scale, every step towards more sustainable world is a step towards right direction.

In summary, based on technical performance alone, developing practical biocolorant solutions for engineering materials is entirely possible. Even though all biocolorants are not suited for every application, biocoloration can provide engineering materials with good color quality, adequate lightfastness and even functional advantages. Importantly, when developing biocolored engineering materials, special attention must be given to preliminary testing during material selection to avoid unexpected phenomena, such as pigment agglomeration of accelerated photodegradation. Therefore, to obtain more practical knowledge on this promising but still rather unexplored field, conducting further experiments on molecular level and exploring new applications are highly encouraged for adventurous researchers and entrepreneurs. As it stands, the continuously growing demand for sustainable engineering is unlikely to seize in the near future. Thus, developing particularly innovative, sustainable, and practical biocolorant solutions may very well result in meaningful to ecological, societal and perhaps even individual benefits.

References

[1] Towns, A. Colorants: General Survey. *Physical Sciences Reviews*, **2019**, *4* (8). https://doi.org/doi:10.1515/psr-2019-0008.

[2] Rohde, H.; Rubio-Fernandez, P. Color Interpretation Is Guided by Informativity Expectations, Not by World Knowledge about Colors. *J Mem Lang*, **2022**, *127*, 104371. https://doi.org/https://doi.org/10.1016/j.jml.2022.104371.

[3] Divers, E. Theory to Practice: Pleasure-Arousal-Dominance (PAD) Theory for Architectural Color Design. *Color Res Appl*, **2023**, *48* (5), 445–452. https://doi.org/https://doi.org/10.1002/col.22847.

[4] Coburn, A.; Kardan, O.; Kotabe, H.; Steinberg, J.; Hout, M. C.; Robbins, A.; MacDonald, J.; Hayn-Leichsenring, G.; Berman, M. G. Psychological Responses to Natural Patterns in Architecture. *J Environ Psychol*, **2019**, *62*, 133–145. https://doi.org/10.1016/j.jenvp.2019.02.007.

[5] Wogalter, M. S.; Mayhorn, C. B.; Zielinska, O. A. Use of Color in Warnings. In *Handbook of Color Psychology*; Cambridge University Press, 2016; pp 377–400. https://doi.org/10.1017/cbo9781107337930.019.

[6] McLellan, G.; Franz, J.; Guaralda, M. The Emergence of the Environmental Color Design Praxis Framework. *Color Res Appl*, **2023**, *48* (5), 639–652. https://doi.org/10.1002/col.22881.

[7] Zhang, H. 1 - Introduction. In *Building Materials in Civil Engineering*; Zhang, H., Ed.; Woodhead Publishing, 2011; pp 1–423. https://doi.org/https://doi.org/10.1533/9781845699567.1.

[8] Fortune Business Insights. *Dyes and Pigments Market Size, Share & Industry Analysis*; 2024.

[9] Colorants Market Size, Share | Global Industry Analysis Report, 2025 https://www.grandviewresearch.com/industry-analysis/colorants-market (accessed Apr 14, 2021).

[10] Lu, Y.; Shao, Y.; Qu, R.; Zheng, C.; Zhang, Y.; Lin, W.; Wu, W.; Feng, Y.; Gao, X. Component Characteristics and Emission Factors of Volatile Organic Compounds from Dyestuff Production. *Aerosol Air Qual Res*, **2020**, *20* (1), 108–118. https://doi.org/10.4209/aaqr.2019.09.0474.

[11] Chequer, F. M. D. Textile Dyes: Dyeing Process and Environmental Impact; Oliveira, G. A. R. de, Ed.; IntechOpen: Rijeka, 2013; p Ch. 6. https://doi.org/10.5772/53659.

[12] Pargai, D.; Jahan, S.; Gahlot, M. Functional Properties of Natural Dyed Textiles. In *Chemistry and Technology of Natural and Synthetic Dyes and Pigments*; IntechOpen, 2020. https://doi.org/10.5772/intechopen.88933.

[13] Akhtar, M. F.; Ashraf, M.; Javeed, A.; Anjum, A. A.; Sharif, A.; Saleem, A.; Akhtar, B.; Khan, A. M.; Altaf, I. Toxicity Appraisal of Untreated Dyeing Industry Wastewater Based on Chemical Characterization and Short Term Bioassays. *Bull Environ Contam Toxicol*, **2016**, *96* (4), 502–507. https://doi.org/10.1007/s00128-016-1759-x.

[14] Fan, J.; Wu, S.; Wang, Z.; Zheng, M.; Zhang, M.; Zhang, L.; Zhong, Y.; Sui, X.; Xu, H.; Mao, Z. Rapid Decolorisation of Dyeing Wastewater by FeIII(2,2′:6′,2″-Terpyridine)Activated Peroxymonosulphate. *Coloration Technology*, **2024**, *140* (2), 300–312. https://doi.org/10.1111/cote.12710.

[15] Gupta, V. K.; Suhas. Application of Low-Cost Adsorbents for Dye Removal - A Review. *Journal of Environmental Management*. Academic Press 2009, pp 2313–2342. https://doi.org/10.1016/j.jenvman.2008.11.017.

[16] Zhao, Y.; Qamar, S. A.; Qamar, M.; Bilal, M.; Iqbal, H. M. N. Sustainable Remediation of Hazardous Environmental Pollutants Using Biochar-Based Nanohybrid Materials. *J Environ Manage*, **2021**, *300*, 113762. https://doi.org/https://doi.org/10.1016/j.jenvman.2021.113762.

[17] Saba, B.; Kjellerup, B. V; Christy, A. D. Eco-Friendly Bio-Electro-Degradation of Textile Dyes Wastewater. *Bioresour Technol Rep*, **2021**, *15*, 100734. https://doi.org/https://doi.org/10.1016/j.biteb.2021.100734.

[18] Hui, M.; Shengyan, P.; Yaqi, H.; Rongxin, Z.; Anatoly, Z.; Wei, C. A Highly Efficient Magnetic Chitosan “Fluid” Adsorbent with a High Capacity and Fast Adsorption Kinetics for Dyeing Wastewater Purification. *Chemical Engineering Journal*, **2018**, *345*, 556–565. https://doi.org/10.1016/j.cej.2018.03.115.

[19] Hinsch, E.; Robinson, S. Comparing Colorfastness to Light of Wood-Staining Fungal Pigments and Commercial Dyes: An Alternative Light Test Method for Color Fastness. *Coatings*, **2018**, *8*, 189. https://doi.org/10.3390/coatings8050189.

[20] Benucci, I.; Lombardelli, C.; Mazzocchi, C.; Esti, M. Natural Colorants from Vegetable Food Waste: Recovery, Regulatory Aspects, and Stability—A Review. *Compr Rev Food Sci Food Saf*, **2022**, *21* (3), 2715–2737. https://doi.org/10.1111/1541-4337.12951.

[21] Gul, R.; Kumar, R.; Sharma, A. K. The Microbial World of Biocolor Production. In *Bio-pigmentation and Biotechnological Implementations*; John Wiley & Sons, Ltd, 2017; pp 263–277. https://doi.org/https://doi.org/10.1002/9781119166191.ch12.

[22] Arora, J.; Agarwal, P.; Gupta, G. Rainbow of Natural Dyes on Textiles Using Plants Extracts: Sustainable and Eco-Friendly Processes. *Green and Sustainable Chemistry*, **2017**, *07* (01), 35–47. https://doi.org/10.4236/gsc.2017.71003.

[23] Chattopadhyay, P.; Chatterjee, S.; Sen, S. K. Biotechnological Potential of Natural Food Grade Biocolorants. *Afr J Biotechnol*, **2008**, *7*.

[24] Křížová, H. Natural Dyes: Their Past, Present, Future and Sustainability. In *Recent Developments in Fibrous Material Science*; OPS, 2015; pp 59–71.

[25] Ferreira, E. S. B.; Hulme, A. N.; McNab, H.; Quye, A. The Natural Constituents of Historical Textile Dyes. *Chem Soc Rev*, **2004**, *33* (6), 329–336. https://doi.org/10.1039/b305697j.

[26] Melo, M. J. History of Natural Dyes in the Ancient Mediterranean Civilization. In *Handbook of Natural Colorants*; John Wiley & Sons, Ltd, 2023; pp 3–26. https://doi.org/https://doi.org/10.1002/9781119811749.ch1.

[27] Abel, A. The History of Dyes and Pigments. In *Colour Design*; Elsevier, 2012; pp 557–587. https://doi.org/10.1016/b978-0-08-101270-3.00024-2.

[28] Potts, D. T. On the History of Madder (Rubia Peregrina L., and Rubia Tinctorum L.) in Pre-Modern Iran and the Caucasus. *Asiatische Studien - Études Asiatiques*, **2022**, *76* (4), 785–819. https://doi.org/10.1515/asia-2021-0039.

[29] Abdel-Kareem, O. History of Dyes Used in Different Historical Periods of Egypt. *Research Journal of Textile and Apparel*, **2012**, *16* (4), 79–92. https://doi.org/10.1108/RJTA-16-04-2012-B009.

[30] Travis, A. S. Anilines: Historical Background. *The Chemistry of Anilines*. February 16, 2007, pp 1–73. https://doi.org/https://doi.org/10.1002/9780470871737.ch1.

[31] Shahid, M.; Shahid-ul-Islam; Mohammad, F. Recent Advancements in Natural Dye Applications: A Review. *J Clean Prod*, **2013**, *53*, 310–331. https://doi.org/10.1016/j.jclepro.2013.03.031.

[32] Harsito, C.; Prabowo, A. R.; Prasetyo, S. D.; Arifin, Z. Enhancement Stability and Color Fastness of Natural Dye: A Review. *Open Engineering*. De Gruyter Open Ltd January 1, 2021, pp 548–555. https://doi.org/10.1515/eng-2021-0055.

[33] Nambela, L.; Haule, L. V.; Mgani, Q. A Review on Source, Chemistry, Green Synthesis and Application of Textile Colorants. *J Clean Prod*, **2020**, *246*, 119036. https://doi.org/https://doi.org/10.1016/j.jclepro.2019.119036.

[34] Affat, S. Classifications, Advantages, Disadvantages, Toxicity Effects of Natural and Synthetic Dyes: A Review. **2021**, *8*, 130–135.

[35] Yadav, S.; Tiwari, K. S.; Gupta, C.; Tiwari, M. K.; Khan, A.; Sonkar, S. P. A Brief Review on Natural Dyes, Pigments: Recent Advances and Future Perspectives. *Results Chem*, **2023**, *5*, 100733. https://doi.org/https://doi.org/10.1016/j.rechem.2022.100733.

[36] Pranta, A. D.; Rahaman, T. Extraction of Eco-Friendly Natural Dyes and Biomordants for Textile Coloration: A Critical Review. *Nano-Structures and Nano-Objects*. Elsevier B.V. September 1, 2024. https://doi.org/10.1016/j.nanoso.2024.101243.

[37] Gürses Ahmet and Açkyldz, M. and G. K. and G. M. S. Dyes and Pigments: Their Structure and Properties. In *Dyes and Pigments*; Springer International Publishing: Cham, 2016; pp 13–29. https://doi.org/10.1007/978-3-319-33892-7_2.

[38] Miller, D. The Physics of Vision. *Biophys Rev Lett*, **2014**, *09*, 135–158. https://doi.org/10.1142/S1793048014310018.

[39] Hurlbert, A.; Ling, Y. 7 - Understanding Colour Perception and Preference. In *Colour Design (Second Edition)*; Best, J., Ed.; Woodhead Publishing Series in Textiles; Woodhead Publishing, 2017; pp 169–192. https://doi.org/https://doi.org/10.1016/B978-0-08-101270-3.00007-2.

[40] In Search of Colour Mechanisms in the Eye and the Brain. In *Foundations of Colour Science*; John Wiley & Sons, Ltd, 2022; pp 317–350. https://doi.org/https://doi.org/10.1002/9781119885955.ch13.

[41] Stockman, A.; Brainard, D. H. Fundamentals of Color Vision I: Color Processing in the Eye. In *Handbook of Color Psychology*; Cambridge University Press, 2016; pp 27–69. https://doi.org/10.1017/cbo9781107337930.004.

[42] Rizzi, A.; Bonanomi, C. 2 - The Human Visual System Described through Visual Illusions. In *Colour Design (Second Edition)*; Best, J., Ed.; Woodhead Publishing Series in Textiles; Woodhead Publishing, 2017; pp 23–41. https://doi.org/https://doi.org/10.1016/B978-0-08-101270-3.00002-3.

[43] Rodriguez-Carmona, M.; Barbur, J. L. 3 - Variability in Normal and Defective Colour Vision: Consequences for Occupational Environments. In *Colour Design (Second Edition)*; Best, J., Ed.; Woodhead Publishing Series in Textiles; Woodhead Publishing, 2017; pp 43–97. https://doi.org/https://doi.org/10.1016/B978-0-08-101270-3.00003-5.

[44] Hanson, A. R. 1 - What Is Colour? In *Colour Design (Second Edition)*; Best, J., Ed.; Woodhead Publishing Series in Textiles; Woodhead Publishing, 2012; pp 3–21. https://doi.org/https://doi.org/10.1016/B978-0-08-101270-3.00001-1.

[45] Object-Colour Stimulus Manifold. In *Foundations of Colour Science*; John Wiley & Sons, Ltd, 2022; pp 375–388. https://doi.org/https://doi.org/10.1002/9781119885955.ch16.

[46] Loe, D. L. 15 - Light, Colour and Human Response. In *Colour Design (Second Edition)*; Best, J., Ed.; Woodhead Publishing Series in Textiles; Woodhead Publishing, 2017; pp 349–369. https://doi.org/https://doi.org/10.1016/B978-0-08-101270-3.00015-1.

[47] Object Colour. In *Foundations of Colour Science*; John Wiley & Sons, Ltd, 2022; pp 351–355. https://doi.org/https://doi.org/10.1002/9781119885955.part2.

[48] Dedrick, D. Some Philosophical Questions about Color. In *Handbook of Color Psychology*; Cambridge University Press, 2016; pp 131–146. https://doi.org/10.1017/cbo9781107337930.007.

[49] Witzel, C.; Hansen, T. Memory Effects on Color Perception. In *Handbook of Color Psychology*; Cambridge University Press, 2016; pp 641–659. https://doi.org/10.1017/cbo9781107337930.032.

[50] Raman, C. D.; Kanmani, S. Textile Dye Degradation Using Nano Zero Valent Iron: A Review. *J Environ Manage*, **2016**, *177*, 341–355. https://doi.org/https://doi.org/10.1016/j.jenvman.2016.04.034.

[51] Chakraborty, J. N. 2 - Colouring Materials. In *Fundamentals and Practices in Colouration of Textiles*; Chakraborty, J. N., Ed.; Woodhead Publishing India, 2010; pp 11–19. https://doi.org/https://doi.org/10.1533/9780857092823.11.

[52] Nassau, K. Chapter 4 - The Fifteen Causes of Color. In *Color for Science, Art and Technology*; Nassau, K., Ed.; AZimuth; North-Holland, 1998; Vol. 1, pp 123–168. https://doi.org/https://doi.org/10.1016/S1387-6783(98)80007-X.

[53] Sen, S.; Deupi, X. Study of Photoselectivity in Linear Conjugated Chromophores Using the XMS-CASPT2 Method. *ACS Physical Chemistry Au*, **2024**. https://doi.org/10.1021/acsphyschemau.4c00065.

[54] Palczewski, K.; Kiser, P. D. Shedding New Light on the Generation of the Visual Chromophore. *Proceedings of the National Academy of Sciences of the United States of America*. National Academy of Sciences August 1, 2020, pp 19629–19638. https://doi.org/10.1073/PNAS.2008211117.

[55] Binjie, X.; Hu, J. 6 - Fabric Appearance Testing. In *Fabric Testing*; Hu, J., Ed.; Woodhead Publishing Series in Textiles; Woodhead Publishing, 2008; pp 148–188. https://doi.org/https://doi.org/10.1533/9781845695064.148.

[56] Bullock, L. Reflectance Spectrophotometry for Measurement of Colour Change. *National Gallery Technical Bulletin*, **1978**, *2*, 48–55.

[57] Badiane, A.; i de Lanuza, G.; Garcia-Custodio, M.; Carazo, P.; Font, E. Color Patch Size and Measurement Error Using Reflectance Spectrophotometry. *Methods Ecol Evol*, **2017**, *8*. https://doi.org/10.1111/2041-210X.12801.

[58] Clarke, P. J. 3 - Instrumental Colour Measurement. In *Total Colour Management in Textiles*; Xin, J. H., Ed.; Woodhead Publishing Series in Textiles; Woodhead Publishing, 2006; pp 44–56. https://doi.org/https://doi.org/10.1533/9781845691080.44.

[59] Goodman, T. M. 18 - International Standards for Colour. In *Colour Design (Second Edition)*; Best, J., Ed.; Woodhead Publishing Series in Textiles; Woodhead Publishing, 2012; pp 417–452. https://doi.org/https://doi.org/10.1016/B978-0-08-101270-3.00018-7.

[60] Setchell, J. S. 4 - Colour Description and Communication. In *Colour Design (Second Edition)*; Best, J., Ed.; Woodhead Publishing Series in Textiles; Woodhead Publishing, 2012; pp 99–129. https://doi.org/https://doi.org/10.1016/B978-0-08-101270-3.00004-7.

[61] Identification of Grassmann Structures Based on Metameric Matching. In *Foundations of Colour Science*; John Wiley & Sons, Ltd, 2022; pp 73–92. https://doi.org/https://doi.org/10.1002/9781119885955.ch3.

[62] Fairchild, M. D. Color Models and Systems. In *Handbook of Color Psychology*; Cambridge University Press, 2016; pp 9–26. https://doi.org/10.1017/cbo9781107337930.003.

[63] Schindler, W. D.; Hauser, P. J. 13 - Finishes to Improve Colour Fastness. In *Chemical Finishing of Textiles*; Schindler, W. D., Hauser, P. J., Eds.; Woodhead Publishing Series in Textiles; Woodhead Publishing, 2004; pp 144–156. https://doi.org/https://doi.org/10.1533/9781845690373.144.

[64] Richards, P. R. Chapter 19 - Fabric Finishing: Dyeing and Colouring. In *Textiles and Fashion*; Sinclair, R., Ed.; Woodhead Publishing Series in Textiles; Woodhead Publishing, 2015; pp 475–505. https://doi.org/https://doi.org/10.1016/B978-1-84569-931-4.00019-2.

[65] Chakraborty, J. N. 29 - Assessment of Fastness of Dyeings. In *Fundamentals and Practices in Colouration of Textiles*; Chakraborty, J. N., Ed.; Woodhead Publishing India, 2010; pp 326–339. https://doi.org/https://doi.org/10.1533/9780857092823.326.

[66] Best, J. 19 - Colour Specification and Visual Approval Methods for Textiles. In *Colour Design (Second Edition)*; Best, J., Ed.; Woodhead Publishing Series in Textiles; Woodhead

Publishing, 2012; pp 453–473. https://doi.org/https://doi.org/10.1016/B978-0-08-101270-3.00019-9.

[67] Chakraborty, J. N. 6 - An Overview of Dye Fastness Testing. In *Woodhead Publishing Series in Textiles*; Clark, M. B. T.-H. of T. and I. D., Ed.; Woodhead Publishing, 2011; Vol. 1, pp 207–224. https://doi.org/https://doi.org/10.1533/9780857093974.1.207.

[68] Easton, J. R. 6 - Key Sustainability Issues in Textile Dyeing. In *Sustainable Textiles*; Blackburn, R. S., Ed.; Woodhead Publishing Series in Textiles; Woodhead Publishing, 2009; pp 139–154. https://doi.org/https://doi.org/10.1533/9781845696948.1.139.

[69] Collett, M.; Cluver, B.; Chen, H. L. Consumer Perceptions the Limited Lifespan of Fast Fashion Apparel. *Research Journal of Textile and Apparel*, **2013**, *17* (2), 61–68. https://doi.org/10.1108/RJTA-17-02-2013-B009.

[70] Laitala, K.; Boks, C.; Klepp, I. G. Making Clothing Last: A Design Approach for Reducing the Environmental Impacts. *International Journal of Design*, **2015**, *9* (2), 93–107.

[71] Sekki, S.; Kauppinen-Räisänen, H.; Kylkilahti, E.; Autio, M. Packaging Journey from Retail to Home: How the Meaning of Sustainability for Colour Transforms. *International Journal of Retail & Distribution Management*, **2023**, *51* (13), 47–63. https://doi.org/10.1108/IJRDM-12-2021-0579.

[72] Dolanbay Doğan, S. A Research on Colours and Fastness Values of Different Materials Dyed with Some Natural Dyes. *International Journal of Materials Science and Applications*, **2018**, *7* (3), 69. https://doi.org/10.11648/j.ijmsa.20180703.11.

[73] Groeneveld, I.; Kanelli, M.; Ariese, F.; van Bommel, M. R. Parameters That Affect the Photodegradation of Dyes and Pigments in Solution and on Substrate – An Overview. *Dyes and Pigments*. Elsevier Ltd February 1, 2023. https://doi.org/10.1016/j.dyepig.2022.110999.

[74] Batchelor, S. N.; Carr, D.; Coleman, C. E.; Fairclough, L.; Jarvis, A. The Photofading Mechanism of Commercial Reactive Dyes on Cotton. *Dyes and Pigments*, **2003**, *59* (3), 269–275. https://doi.org/10.1016/S0143-7208(03)00118-9.

[75] Oakes, J. Photofading of Textile Dyes. *Review of Progress in Coloration and Related Topics*, **2001**, *32*, 21–28. https://doi.org/10.1111/j.1478-4408.2001.tb00134.x.

[76] Mamun Kabir, S. M.; Raafi, S.; Koh, J. Photofading Mechanism of Reactive Blue Dyes on Cotton against Sunlight and Xenon-Arc Lamp. *Journal of Textile and Apparel, Technology and Management*, **2020**, *11*, 2020.

[77] Auger, J.-C.; McLoughlin, D. Experimental and Theoretical Studies of Perceptible Color Fading of Decorative Paints Consisting of Mixed Pigments. *J Quant Spectrosc Radiat Transf*, **2017**, *187*, 322–332. https://doi.org/https://doi.org/10.1016/j.jqsrt.2016.10.012.

[78] Saville, B. P. 9 - Colour Fastness Testing. In *Physical Testing of Textiles*; Saville, B. P., Ed.; Woodhead Publishing Series in Textiles; Woodhead Publishing, 1999; pp 244–255. https://doi.org/https://doi.org/10.1533/9781845690151.244.

[79] Bide, M. 9 - Colour Measurement and Fastness Assessment. In *Colour Measurement*; Gulrajani, M. L., Ed.; Woodhead Publishing Series in Textiles; Woodhead Publishing, 2010; pp 196–217. https://doi.org/https://doi.org/10.1533/9780857090195.1.196.

[80] Clark, R. J. H.; Cooksey, C. J.; Daniels, M. A. M.; Withnall, R. Indigo, Woad, and Tyrian Purple: Important Vat Dyes from Antiquity to the Present. *Endeavour*, **1993**, *17* (4). https://doi.org/10.1016/0160-9327(93)90062-8.

[81] Sharif, S.; Nabais, P.; Melo, M. J.; Pina, F.; Oliveira, M. C. Photoreactivity and Stability of Flavonoid Yellows Used in Cultural Heritage. *Dyes and Pigments*, **2022**, *199*, 110051. https://doi.org/https://doi.org/10.1016/j.dyepig.2021.110051.

[82] Püntener, A.; Schlesinger, U. 9 - Natural Dyes. In *Colorants for Non-Textile Applications*; Freeman, H. S., Peters, A. T., Eds.; Elsevier Science: Amsterdam, 2000; pp 382–455. https://doi.org/https://doi.org/10.1016/B978-044482888-0/50040-4.

[83] Pattanaik, L.; Padhi, S. K.; Hariprasad, P.; Naik, S. N. Life Cycle Cost Analysis of Natural Indigo Dye Production from Indigofera Tinctoria L. Plant Biomass: A Case Study of India. *Clean Technol Environ Policy*, **2020**, *22* (8), 1639–1654. https://doi.org/10.1007/s10098-020-01914-y.

[84] Bechtold, T.; Mahmud-Ali, A.; Mussak, R. 19 - Natural Dyes from Food Processing Wastes. In *Handbook of Waste Management and Co-Product Recovery in Food Processing*; Waldron, K., Ed.; Woodhead Publishing Series in Food Science, Technology and Nutrition; Woodhead Publishing, 2007; pp 502–533. https://doi.org/https://doi.org/10.1533/9781845692520.4.502.

[85] Hill, D. J. Is There a Future for Natural Dyes? *Review of Progress in Coloration and Related Topics*, **1997**, *27* (1), 18–25. https://doi.org/https://doi.org/10.1111/j.1478-4408.1997.tb03771.x.

[86] Geissler, S.; Bechtold, T. Environmental and Economic Position of Natural Colorants—Energy and Resources Balances, Sustainability, Ecology, and Costs. In *Handbook of Natural Colorants*; John Wiley & Sons, Ltd, 2023; pp 591–612. https://doi.org/https://doi.org/10.1002/9781119811749.ch29.

[87] Bechtold, T.; Pham, T.; Manian, A. P. Sources for Natural Colorants in Europe. In *Handbook of Natural Colorants*; John Wiley & Sons, Ltd, 2023; pp 45–61. https://doi.org/https://doi.org/10.1002/9781119811749.ch4.

[88] Glatard, F.; de la Sayette, A.; Fertet, A. Large-Scale Cultivation of Two Dye Plants: Madder (Rubia Tinctorum L.) and Weld (Reseda Luteola L.). In *Acta Horticulturae*; International Society for Horticultural Science, 2023; Vol. 1361, pp 31–38. https://doi.org/10.17660/ActaHortic.2023.1361.4.

[89] John, P.; Angelini, L. G. Indigo—Production and Properties. In *Handbook of Natural Colorants*; John Wiley & Sons, Ltd, 2023; pp 195–250. https://doi.org/https://doi.org/10.1002/9781119811749.ch11.

[90] John, P.; Angelini, L. G. Indigo – Agricultural Aspects. *Handbook of Natural Colorants*. April 17, 2009, pp 73–104. https://doi.org/https://doi.org/10.1002/9780470744970.ch7.

[91] Blackburn, R. S.; Bechtold, T.; John, P. The Development of Indigo Reduction Methods and Pre-Reduced Indigo Products. *Coloration Technology*. 2009, pp 193–207. https://doi.org/10.1111/j.1478-4408.2009.00197.x.

[92] Samanta, A. K.; Singhee, D. Sources, Application, and Analysis of Natural Colorants: An Indian Perspective. In *Handbook of Natural Colorants*; John Wiley & Sons, Ltd, 2023; pp 103–159. https://doi.org/https://doi.org/10.1002/9781119811749.ch8.

[93] John, P. Indigo – Extraction. *Handbook of Natural Colorants*. April 17, 2009, pp 105–133. https://doi.org/https://doi.org/10.1002/9780470744970.ch8.

[94] Lohtander, T.; Durandin, N.; Laaksonen, T.; Arola, S.; Laaksonen, P. Stabilization of Natural and Synthetic Indigo on Nanocellulose Network - Towards Bioactive Materials and Facile Dyeing Processes. *J Clean Prod*, **2021**, *328*. https://doi.org/10.1016/j.jclepro.2021.129615.

[95] Mocquard, J.; Le Lamer, A.-C.; Fabre, P.-L.; Mathieu, C.; Chastrette, C.; Vitrai, A.; Vandenbossche, V. Indigo Dyeing from Isatis Tinctoria L.: From Medieval to Modern Use. *Dyes and Pigments*, **2022**, *207*, 110675. https://doi.org/https://doi.org/10.1016/j.dyepig.2022.110675.

[96] Maugard, T.; Enaud, E.; Choisy, P.; Legoy, M. D. Identification of an Indigo Precursor from Leaves of Isatis Tinctoria (Woad). *Phytochemistry*, **2001**, *58* (6), 897–904. https://doi.org/https://doi.org/10.1016/S0031-9422(01)00335-1.

[97] Novotná, P.; Boon, J. J.; van der Horst, J.; Pacáková, V. Photodegradation of Indigo in Dichloromethane Solution. *Coloration Technology*, **2003**, *119* (3), 121–127. https://doi.org/10.1111/j.1478-4408.2003.tb00161.x.

[98] Hartl, A.; Proaño Gaibor, A. N.; van Bommel, M. R.; Hofmann-de Keijzer, R. Searching for Blue: Experiments with Woad Fermentation Vats and an Explanation of the Colours through Dye Analysis. *J Archaeol Sci Rep*, **2015**, *2*, 9–39. https://doi.org/https://doi.org/10.1016/j.jasrep.2014.12.001.

[99] Saikhao, L.; Setthayanond, J.; Karpkird, T.; Suwanruji, P. Comparison of Sodium Dithionite and Glucose as a Reducing Agent for Natural Indigo Dyeing on Cotton Fabrics. *MATEC Web of Conferences*, **2017**, *108* (03001). https://doi.org/10.1051/matecconf/201710803001.

[100] Rai, S.; Saremi, R.; Sharma, S.; Minko, S. Environment-Friendly Nanocellulose-Indigo Dyeing of Textiles. *Green Chemistry*, **2021**, *23* (20), 7937–7944. https://doi.org/10.1039/d1gc02043a.

[101] Ben Ticha, M.; Meksi, N.; Drira, N.; Kechida, M.; Mhenni, M. F. A Promising Route to Dye Cotton by Indigo with an Ecological Exhaustion Process: A Dyeing Process Optimization Based on a Response Surface Methodology. *Ind Crops Prod*, **2013**, *46*, 350–358. https://doi.org/10.1016/j.indcrop.2013.02.009.

[102] Luo, Y.; Pei, L.; Wang, J. Sustainable Indigo Dyeing and Improvement of Rubbing Fastness of Dyed Cotton Fiber Using Different Fixing Agents for Obtaining Eco-Friendly Cowboy Products. *J Clean Prod*, **2020**, *251*. https://doi.org/10.1016/j.jclepro.2019.119728.

[103] Seixas De Melo, J.; Moura, A. P.; Melo, M. J. Photophysical and Spectroscopic Studies of Indigo Derivatives in Their Keto and Leuco Forms. *Journal of Physical Chemistry A*, **2004**, *108* (34), 6975–6981. https://doi.org/10.1021/jp049076y.

[104] Splitstoser, J.; Dillehay, T.; Wouters, J.; Claro, A. Early Pre-Hispanic Use of Indigo Blue in Peru. *Sci Adv*, **2016**, *2*, e1501623–e1501623. https://doi.org/10.1126/sciadv.1501623.

[105] Padfield, T.; Landi, S. The Light-Fastness of the Natural Dyes. *Studies in Conservation*, **1966**, *11* (4), 181–196. https://doi.org/10.1179/sic.1966.022.

[106] Jordan, J.; Laaksonen, P. Color Stability of Polylactic Acid Pigmented with Natural Indigo of Isatis Tinctoria in Artificial Weathering. In *XXXI International Horticultural Congress (IHC2022): International Symposium on Natural Colourants*; Acta Horticulturae, 2023.

[107] Reningtyas, R.; Rahayuningsih, E.; Kusumastuti, Y.; Kartini, I. Photofading of Natural Indigo Dye in Cotton Coated with Zinc Oxide Nanoparticles Synthesized by Precipitation Method. *International Journal of Technology*, **2022**, *13* (3), 553–564. https://doi.org/10.14716/ijtech.v13i3.4756.

[108] Do, K. L.; Mushtaq, A.; Zhao, F.; Su, M. Alizarin Old and New: Extraction Techniques for Coloration, Advances in Detection Methods for Historical Textiles and Novel Applications as a Functional Dye. *Coloration Technology*. John Wiley and Sons Inc February 1, 2024, pp 5–29. https://doi.org/10.1111/cote.12711.

[109] Derksen, G. C. H.; Bechtold, T. Natural Colorants—Quinoid, Naphthoquinoid, and Anthraquinoid Dyes. In *Handbook of Natural Colorants*; John Wiley & Sons, Ltd, 2023; pp 271–315. https://doi.org/https://doi.org/10.1002/9781119811749.ch13.

[110] Derksen, G. C. H.; van Holthoon, F. L.; Willemen, H. M.; Krul, C. A. M.; Franssen, M. C. R.; van Beek, T. A. Development of a Process for Obtaining Non-Mutagenic Madder Root (Rubia Tinctorum) Extract for Textile Dyeing. *Ind Crops Prod*, **2021**, *164*. https://doi.org/10.1016/j.indcrop.2021.113344.

[111] Brunet, C.; de la Sayette, A. Natural Pigments for (Bio)-Plastics Colouring. In *Acta Horticulturae*; International Society for Horticultural Science, 2023; Vol. 1361, pp 149–162. https://doi.org/10.17660/ActaHortic.2023.1361.17.

[112] Jiang, H. Y.; Hu, X. D.; Zhu, J. J.; Wan, J.; Yao, J. B. Studies on the Photofading of Alizarin, the Main Component of Madder. *Dyes and Pigments*, **2021**, *185*. https://doi.org/10.1016/j.dyepig.2020.108940.

[113] Abou Elmaaty, T.; Sayed-Ahmed, K.; Magdi, M.; Elsisi, H. An Eco-Friendly Method of Extracting Alizarin from Rubia Tinctorum Roots under Supercritical Carbon Dioxide and

Its Application to Wool Dyeing. *Sci Rep*, **2023**, *13* (1). https://doi.org/10.1038/s41598-022-27110-0.

[114] Mikropoulou, E.; Tsatsaroni, E.; Varella, E. A. Revival of Traditional European Dyeing Techniques Yellow and Red Colorants. *J Cult Herit*, **2009**, *10* (4), 447–457. https://doi.org/10.1016/j.culher.2009.02.003.

[115] Deveoglu, O.; Sahinbaskan, B. Y.; Torgan, E.; Karadag, R. Investigation on Colour, Fastness Properties and HPLC-DAD Analysis of Silk Fibres Dyed with Rubia Tinctorium L. and Quercus Ithaburensis Decaisne. *Coloration Technology*, **2012**, *128* (5), 364–370. https://doi.org/https://doi.org/10.1111/j.1478-4408.2012.00389.x.

[116] Farias, N. O. de; Albuquerque, A. F. de; dos Santos, A.; Almeida, G. C. F.; Freeman, H. S.; Räisänen, R.; Umbuzeiro, G. de A. Is Natural Better? An Ecotoxicity Study of Anthraquinone Dyes. *Chemosphere*, **2023**, *343*. https://doi.org/10.1016/j.chemosphere.2023.140174.

[117] Shahi, Z.; Mehrizi, M. K.; Hadizadeh, M. A Review of the Natural Resources Used to Hair Color and Hair Care Products. *Journal of Pharmaceutical Sciences and Research*, **2017**, *9* (7), 1026–1030.

[118] Ozen, E.; Yeniocak, M.; Goktas, O.; Hakkı Alma, M.; Yilmaz, F. Antimicrobial and Antifungal Properties of Madder Root (Rubia Tinctorum) Colorant Used as an Environmentally-Friendly Wood Preservative. *Bioresources*, **2014**, *9* (2). https://doi.org/10.15376/biores.9.2.1998-2009.

[119] Raza Naqvi, S. A.; Kaif ul-Wara; Adeel, S.; Mia, R.; Hosseinnezhad, M.; Rather, L. J.; Imran, M. Modern Ecofriendly Approach for Extraction of Luteolin Natural Dye from Weld for Silk Fabric and Wool Yarn Dyeing. *Sustain Chem Pharm*, **2024**, *39*. https://doi.org/10.1016/j.scp.2024.101554.

[120] Li, R.; Zhou, Y.; Zhang, S.; Li, J.; Zheng, Y.; Fan, X. The Natural (Poly)Phenols as Modulators of Microglia Polarization via TLR4/NF-KB Pathway Exert Anti-Inflammatory Activity in Ischemic Stroke. *European Journal of Pharmacology*. Elsevier B.V. January 5, 2022. https://doi.org/10.1016/j.ejphar.2021.174660.

[121] Liu, C.; Ma, X.; Zhuang, J.; Liu, L.; Sun, C. Cardiotoxicity of Doxorubicin-Based Cancer Treatment: What Is the Protective Cognition That Phytochemicals Provide Us? *Pharmacological Research*. Academic Press October 1, 2020. https://doi.org/10.1016/j.phrs.2020.105062.

[122] Karadag, R. Sustainable and Mass Production of Cotton Dyeing with Natural Dye (Weld) in the Textile Industry. *Journal of Natural Fibers*, **2022**, *19* (15), 10935–10945. https://doi.org/10.1080/15440478.2021.2002781.

[123] Angelini, L. G.; Bertoli, A.; Rolandelli, S.; Pistelli, L. Agronomic Potential of Reseda Luteola L. as New Crop for Natural Dyes in Textiles Production. *Ind Crops Prod*, **2003**, *17* (3), 199–207. https://doi.org/10.1016/S0926-6690(02)00099-7.

[124] Cayetano-Salazar, L.; Nava-Tapia, D. A.; Astudillo-Justo, K. D.; Arizmendi-Izazaga, A.; Sotelo-Leyva, C.; Herrera-Martinez, M.; Villegas-Comonfort, S.; Navarro-Tito, N. Flavonoids as Regulators of TIMPs Expression in Cancer: Consequences, Opportunities, and Challenges. *Life Sciences*. Elsevier Inc. November 1, 2022. https://doi.org/10.1016/j.lfs.2022.120932.

[125] Xue, J. C.; Yuan, S.; Meng, H.; Hou, X. T.; Li, J.; Zhang, H. M.; Chen, L. L.; Zhang, C. H.; Zhang, Q. G. The Role and Mechanism of Flavonoid Herbal Natural Products in Ulcerative Colitis. *Biomedicine and Pharmacotherapy*. Elsevier Masson s.r.l. February 1, 2023. https://doi.org/10.1016/j.biopha.2022.114086.

[126] Dumitrescu, I.; Constantinescu, R.; Mitran, E. C.; Perdum, E.; Chirilă, L.; Iordache, O. G.; Ştefănescu, D.; Pîslaru, M.; Mancaşi, I. Antibacterial and Uv Protective Effects of Cotton Fabrics Dyed with Reseda Luteola Extract. In *ICAMS Proceedings of the International*

Conference on Advanced Materials and Systems; Inst. Nat. Cercetare-Dezvoltare Text. Pielarie, 2018; pp 421–426. https://doi.org/10.24264/icams-2018.VIII.6.

[127] Serrano, C.; Sapata, M.; Oliveira, M. C.; Calha, I.; Sá e Melo, L. Stabilization of Luteolins from Weld (Reseda Luteola L.) and Sawwort (Serratula Tinctoria L.) by Microencapsulation for Natural Dyeing. In *Acta Horticulturae*; International Society for Horticultural Science, 2023; Vol. 1361, pp 119–130. https://doi.org/10.17660/ActaHortic.2023.1361.14.

[128] Villela, A.; van Vuuren, M. S. A.; Willemen, H. M.; Derksen, G. C. H.; van Beek, T. A. Photo-Stability of a Flavonoid Dye in Presence of Aluminium Ions. *Dyes and Pigments*, **2019**, *162*, 222–231. https://doi.org/10.1016/j.dyepig.2018.10.021.

[129] Punia Bangar, S.; Kajla, P.; Chaudhary, V.; Sharma, N.; Ozogul, F. Luteolin: A Flavone with Myriads of Bioactivities and Food Applications. *Food Bioscience*. Elsevier Ltd April 1, 2023. https://doi.org/10.1016/j.fbio.2023.102366.

[130] Panouillé, M.; Ralet, M.-C.; Bonnin, E.; Thibault, J.-F. 16 - Recovery and Reuse of Trimmings and Pulps from Fruit and Vegetable Processing. In *Handbook of Waste Management and Co-Product Recovery in Food Processing*; Waldron, K., Ed.; Woodhead Publishing Series in Food Science, Technology and Nutrition; Woodhead Publishing, 2007; pp 417–447. https://doi.org/https://doi.org/10.1533/9781845692520.4.417.

[131] Jameel, M.; Umar, K.; Parveen, T.; Ismail, I. M. I.; Qari, H. A.; Yaqoob, A. A.; Ibrahim, M. N. M. Chapter 12 - Extraction of Natural Dyes from Agro-Industrial Waste. In *Extraction of Natural Products from Agro-Industrial Wastes*; Bhawani, S. A., Khan, A., Ahmad, F. B., Eds.; Elsevier, 2023; pp 197–216. https://doi.org/https://doi.org/10.1016/B978-0-12-823349-8.00018-6.

[132] Räisänen, R.; Primetta, A.; Toukola, P.; Fager, S.; Ylänen, J. Biocolourants from Onion Crop Side Streams and Forest Mushroom for Regenerated Cellulose Fibres. *Ind Crops Prod*, **2023**, *198*, 116748. https://doi.org/https://doi.org/10.1016/j.indcrop.2023.116748.

[133] Rather, L. J.; Zhou, Q.; Ali, A.; Haque, Q. Mohd. R.; Li, Q. Valorization of Agro-Industrial Waste from Peanuts for Sustainable Natural Dye Production: Focus on Adsorption Mechanisms, Ultraviolet Protection, and Antimicrobial Properties of Dyed Wool Fabric. *ACS Food Science & Technology*, **2021**, *1* (3), 427–442. https://doi.org/10.1021/acsfoodscitech.1c00005.

[134] Moreno-González, M.; Ottens, M. A Structured Approach to Recover Valuable Compounds from Agri-Food Side Streams. *Food Bioproc Tech*, **2021**, *14* (8), 1387–1406. https://doi.org/10.1007/s11947-021-02647-6.

[135] Adeel, S.; Azeem, M.; Habib, N.; Hussaan, M.; Kiran, A.; Haji, A.; Haddar, W. Sustainable Application of Microwave Assisted Extracted Tea Based Tannin Natural Dye for Chemical and Bio-Mordanted Wool Fabric. *Journal of Natural Fibers*, **2023**, *20* (1), 2136322. https://doi.org/10.1080/15440478.2022.2136322.

[136] Mongkholrattanasit, R.; Nakpathom, M.; Vuthiganond, N. Eco-Dyeing with Biocolorant from Spent Coffee Ground on Low Molecular Weight Chitosan Crosslinked Cotton. *Sustain Chem Pharm*, **2021**, *20*. https://doi.org/10.1016/j.scp.2021.100389.

[137] Helander, R.; Leppäkoski, S.; Moilanen, U.; Tossavainen, M.; Laaksonen, P. Boreal Forest Side Streams for Natural Colorants and Growing Media. *Sustain Chem Pharm*, **2024**, *39*, 101615. https://doi.org/https://doi.org/10.1016/j.scp.2024.101615.

[138] Melo, M. J.; Pina, F.; Teixeira, N.; Andary, C. Anthocyanins: Revisiting Nature's Glamorous Palette. In *Handbook of Natural Colorants*; John Wiley & Sons, Ltd, 2023; pp 251–270. https://doi.org/https://doi.org/10.1002/9781119811749.ch12.

[139] Rein, M. Copigmentation Reactions and Color Stability of Berry Anthocyanins, University of Helsinki: Helsinki, 2005.

[140] Zuber, M.; Adeel, S.; Rehman, F.-U.; Anjum, F.; Muneer, M.; Abdullah, M.; Zia, K. M. Influence of Microwave Radiation on Dyeing of Bio-Mordanted Silk Fabric Using Neem

Bark (Azadirachta Indica)-Based Tannin Natural Dye. *Journal of Natural Fibers*, **2020**, *17* (10), 1410–1422. https://doi.org/10.1080/15440478.2019.1576569.

[141] Sargsyan, L.; Vill, V.; Hippe, T. Investigations of Vegetable Tannins as Hair Dyes and Their Interactions with Pre-Bleached Hair Fibres. *Int J Cosmet Sci*, **2020**, *42* (4), 320–327. https://doi.org/https://doi.org/10.1111/ics.12624.

[142] Xu, H.; Song, H. A Systematic Review of Tea Dyeing in the Textile Industry: Research Trends, Dyeing Performance, Functional Characteristics, and Application Potential. *AATCC Journal of Research*, **2025**, *12* (1), 24723444251314916. https://doi.org/10.1177/24723444251314916.

[143] Sarker, M. K. U.; Haque, M. M.; Hasan, M. R.; Sultana, S.; Ray, S. K.; Shaikh, M. A. A. Utilization of Factory Tea (Camellia Sinensis) Wastes in Eco-Friendly Dyeing of Jute Packaging Fabrics. *Heliyon*, **2024**, *10* (10), e30948. https://doi.org/https://doi.org/10.1016/j.heliyon.2024.e30948.

[144] Mongkholrattanasit, R.; Nakpathom, M.; Vuthiganond, N. Eco-Dyeing with Biocolorant from Spent Coffee Ground on Low Molecular Weight Chitosan Crosslinked Cotton. *Sustain Chem Pharm*, **2021**, *20*, 100389. https://doi.org/https://doi.org/10.1016/j.scp.2021.100389.

[145] Melaku, A.; Demeke, G.; Aschale, M.; Alemayehu, F.; Semegn, G. Extraction and Characterization of Natural Dye Stuff from Spent Coffee Ground and Bio-Mordant from Mango Bark. *Journal of Natural Fibers*, **2023**, *20*. https://doi.org/10.1080/15440478.2023.2276725.

[146] Xia, W.; Li, Z.; Tang, Y.; Li, Q. Sustainable Recycling of Café Waste as Natural Bio Resource and Its Value Adding Applications in Green and Effective Dyeing/Bio Finishing of Textile. *Sep Purif Technol*, **2023**, *309*, 123091. https://doi.org/https://doi.org/10.1016/j.seppur.2022.123091.

[147] Bechtold, T.; Manian, A. Technical Aspects and Requirements to Produce Natural Colorants—Processes and Product Standardization. In *Handbook of Natural Colorants*; John Wiley & Sons, Ltd, 2023; pp 573–589. https://doi.org/https://doi.org/10.1002/9781119811749.ch28.

[148] Goh, Y.; Lauro, S.; Barber, S. T.; Williams, S. A.; Trabold, T. A. Cleaner Production of Flexographic Ink by Substituting Carbon Black with Biochar. *J Clean Prod*, **2021**, *324*, 129262. https://doi.org/https://doi.org/10.1016/j.jclepro.2021.129262.

[149] Lohtander-Piispa, T. Functional Materials from Cellulose and Biocolorants, Aalto University: Espoo, 2022.

[150] Santos, J.; Monteiro, S.; Oliveira, S.; Magalhães, P.; Magalhães, F. D.; Martins, J. M.; de Carvalho, L. H. Application of Forest By-Products in the Textile Industry: Dyeing with Pine and Eucalyptus Bark Extracts; MDPI AG, 2022; p 30. https://doi.org/10.3390/iecf2022-13053.

[151] Divya, E.; Madhumitha, T.; Nandini, R.; Pooja, R.; Manickam, A.; Bhanu Rekha, V.; Tech, B.; Professor, A. Extraction of Natural Dyes from Forest Trees and Their Application in Textiles. *IJSRD-International Journal for Scientific Research & Development|*, **2013**, *1*.

[152] Kumar, R.; Tripathi, Y. Natural Dyes from Forest Biomass. In *Training Manual on Extraction Technology of Natural Dyes & Aroma Therapy and Cultivation Value Addition of Medicinal Plants*; Forest Research Institute: Dehradun, 2011; pp 51–69. https://doi.org/10.13140/2.1.4934.9927.

[153] Naseer, S.; Afzal, M. S.; Nisa, A.; Hussain, S.; Ahmad, M. A.; Parveen, S.; Anjum, F.; Riaz, M. Extraction of Brown Dye from Eucalyptus Bark and Its Applications in Food Storage. *Quality Assurance and Safety of Crops and Foods*, **2019**, *11* (8), 769–780. https://doi.org/10.3920/QAS2019.1569.

[154] Lohtander, T.; Arola, S.; Laaksonen, P. Biomordanting Willow Bark Dye on Cellulosic Materials. *Coloration Technology*, **2020**, *136* (1), 3–14. https://doi.org/10.1111/cote.12442.

[155] Miranda, I.; Gominho, J.; Mirra, I.; Pereira, H. Chemical Characterization of Barks from Picea Abies and Pinus Sylvestris after Fractioning into Different Particle Sizes. *Ind Crops Prod*, **2012**, *36* (1), 395–400. https://doi.org/https://doi.org/10.1016/j.indcrop.2011.10.035.

[156] Bechtold, T.; Mahmud-Ali, A.; Mussak, R. A. M. Reuse of Ash-Tree (Fraxinus Excelsior L.) Bark as Natural Dyes for Textile Dyeing: Process Conditions and Process Stability. *Coloration Technology*, **2007**, *123* (4), 271–279. https://doi.org/https://doi.org/10.1111/j.1478-4408.2007.00095.x.

[157] Kim, D.; Anderson, N.; Chung, W. Financial Performance of a Mobile Pyrolysis System Used to Produce Biochar from Sawmill Residues. *For Prod J*, **2015**, *65*, 189–197. https://doi.org/10.13073/FPJ-D-14-00052.

[158] Sessa, F.; Veeyee, K. F.; Canu, P. Optimization of Biochar Quality and Yield from Tropical Timber Industry Wastes. *Waste Management*, **2021**, *131*, 341–349. https://doi.org/https://doi.org/10.1016/j.wasman.2021.06.017.

[159] Kohlhuber, N.; Musl, O.; Sulaeva, I.; Böhmdorfer, S.; Sumerskii, I.; Ters, T.; Rosenau, T.; Potthast, A. Adding Speed to Lignin Analysis Straight from Black Liquors. *ACS Sustain Chem Eng*, **2023**, *11* (42), 15294–15301. https://doi.org/10.1021/acssuschemeng.3c03616.

[160] Duangkaew, N.; Lacson, C. F. Z.; Grisdanurak, N.; Neramittagapong, S.; de Luna, M. D. G. Lignin Extraction from Kraft Black Liquor and Its Conversion to Phenol-Rich Oil by Hydrothermal Liquefaction Process. *Bioresour Technol Rep*, **2024**, *25*, 101759. https://doi.org/https://doi.org/10.1016/j.biteb.2023.101759.

[161] Sharma, M.; Marques, J.; Simões, A.; Donato, M. M.; Cardoso, O.; Gando-Ferreira, L. M. Optimization of Lignin Precipitation from Black Liquor Using Organic Acids and Its Valorization by Preparing Lignin Nanoparticles. *Int J Biol Macromol*, **2024**, *269*, 131881. https://doi.org/https://doi.org/10.1016/j.ijbiomac.2024.131881.

[162] Berlin, A.; Balakshin, M. Industrial Lignins: Analysis, Properties, and Applications. In *Bioenergy Research: Advances and Applications*; Elsevier Inc., 2014; pp 315–336. https://doi.org/10.1016/B978-0-444-59561-4.00018-8.

[163] Crestini, C.; Lange, H.; Sette, M.; Argyropoulos, D. S. On the Structure of Softwood Kraft Lignin. *Green Chem.*, **2017**, *19* (17), 4104–4121. https://doi.org/10.1039/C7GC01812F.

[164] Lancefield, C. S.; Wienk, H. L. J.; Boelens, R.; Weckhuysen, B. M.; Bruijnincx, P. C. A. Identification of a Diagnostic Structural Motif Reveals a New Reaction Intermediate and Condensation Pathway in Kraft Lignin Formation. *Chem. Sci.*, **2018**, *9* (30), 6348–6360. https://doi.org/10.1039/C8SC02000K.

[165] Liu, R.; Smeds, A.; Wang, L.; Pranovich, A.; Hemming, J.; Willför, S.; Zhang, H.; Xu, C. Fractionation of Lignin with Decreased Heterogeneity: Based on a Detailed Characteristics Study of Sequentially Extracted Softwood Kraft Lignin. *ACS Sustain Chem Eng*, **2021**, *9* (41), 13862–13873. https://doi.org/10.1021/acssuschemeng.1c04725.

[166] Alekhina, M.; Ershova, O.; Ebert, A.; Heikkinen, S.; Sixta, H. Softwood Kraft Lignin for Value-Added Applications: Fractionation and Structural Characterization. *Ind Crops Prod*, **2015**, *66*, 220–228. https://doi.org/https://doi.org/10.1016/j.indcrop.2014.12.021.

[167] Pajer, N.; Cestari, C.; Argyropoulos, D. S.; Crestini, C. From Lignin Self Assembly to Nanoparticles Nucleation and Growth: A Critical Perspective. *npj Materials Sustainability*, **2024**, *2* (1). https://doi.org/10.1038/s44296-024-00037-5.

[168] Dessbesell, L.; Paleologou, M.; Leitch, M.; Pulkki, R.; Xu, C. (Charles). Global Lignin Supply Overview and Kraft Lignin Potential as an Alternative for Petroleum-Based Polymers. *Renewable and Sustainable Energy Reviews*, **2020**, *123*, 109768. https://doi.org/https://doi.org/10.1016/j.rser.2020.109768.

[169] Liu, R.; Smeds, A.; Willför, S.; Xu, C. Structural Properties of Softwood Lignin Fractions: Revealed by NMR and Py-GC/MS. *Ind Crops Prod*, **2024**, *209*. https://doi.org/10.1016/j.indcrop.2024.118055.

[170] Argyropoulos, D. D. S.; Crestini, C.; Dahlstrand, C.; Furusjö, E.; Gioia, C.; Jedvert, K.; Henriksson, G.; Hulteberg, C.; Lawoko, M.; Pierrou, C.; et al. Kraft Lignin: A Valuable, Sustainable Resource, Opportunities and Challenges. *ChemSusChem*. John Wiley and Sons Inc December 7, 2023. https://doi.org/10.1002/cssc.202300492.

[171] Chio, C.; Sain, M.; Qin, W. Lignin Utilization: A Review of Lignin Depolymerization from Various Aspects. *Renewable and Sustainable Energy Reviews*, **2019**, *107*, 232–249. https://doi.org/https://doi.org/10.1016/j.rser.2019.03.008.

[172] Liu, J.; Li, X.; Li, M.; Zheng, Y. Lignin Biorefinery: Lignin Source, Isolation, Characterization, and Bioconversion. In *Advances in Bioenergy*; Li, Y., Zhou, Y., Eds.; Advances in Bioenergy; Elsevier, 2022; Vol. 7, pp 211–270. https://doi.org/https://doi.org/10.1016/bs.aibe.2022.05.004.

[173] Ponnusamy, V. K.; Nguyen, D. D.; Dharmaraja, J.; Shobana, S.; Banu, J. R.; Saratale, R. G.; Chang, S. W.; Kumar, G. A Review on Lignin Structure, Pretreatments, Fermentation Reactions and Biorefinery Potential. *Bioresour Technol*, **2019**, *271*, 462–472. https://doi.org/https://doi.org/10.1016/j.biortech.2018.09.070.

[174] Lawoko, M.; Samec, J. S. M. Kraft Lignin Valorization: Biofuels and Thermoset Materials in Focus. *Curr Opin Green Sustain Chem*, **2023**, *40*, 100738. https://doi.org/https://doi.org/10.1016/j.cogsc.2022.100738.

[175] Wang, Y. Y.; Wyman, C. E.; Cai, C. M.; Ragauskas, A. J. Lignin-Based Polyurethanes from Unmodified Kraft Lignin Fractionated by Sequential Precipitation. *ACS Appl Polym Mater*, **2019**, *1* (7), 1672–1679. https://doi.org/10.1021/acsapm.9b00228.

[176] Zevallos Torres, L. A.; Lorenci Woiciechowski, A.; de Andrade Tanobe, V. O.; Karp, S. G.; Guimarães Lorenci, L. C.; Faulds, C.; Soccol, C. R. Lignin as a Potential Source of High-Added Value Compounds: A Review. *J Clean Prod*, **2020**, *263*, 121499. https://doi.org/https://doi.org/10.1016/j.jclepro.2020.121499.

[177] Forsman, N.; Lohtander, T.; Jordan, J.; Huynh, N.; Seppälä, A.; Laaksonen, P.; Franssila, S.; Österberg, M. Microalgae Chlorella Vulgaris and Kraft Lignin Stabilized Cellulosic Wet Foams for Camouflage. *Soft Matter*, **2022**, *18* (10), 2060–2071. https://doi.org/10.1039/D1SM01719E.

[178] Hassan, M. M. Valorization of Sulfonated Kraft Lignin as a Natural Dye for the Sustainable Dyeing of Wool Fabrics: Effect of Peroxide Oxidation. *ACS Sustain Chem Eng*, **2023**, *11* (37), 13787–13797. https://doi.org/10.1021/acssuschemeng.3c04267.

[179] Mun, J. S.; Mun, S. P. Potential of Hardwood Kraft Lignin as a Bio-Based Dye for Cotton Fabrics. *Bioresources*, **2023**, *19*, 973–984. https://doi.org/10.15376/biores.19.1.973-984.

[180] Armah, E. K.; Chetty, M.; Adedeji, J. A.; Estrice, D. E.; Mutsvene, B.; Singh, N.; Tshemese, Z. Biochar: Production, Application and the Future. In *Biochar*; Bartoli, M., Giorcelli, M., Tagliaferro, A., Eds.; IntechOpen: Rijeka, 2022. https://doi.org/10.5772/intechopen.105070.

[181] Weber, K.; Quicker, P. Properties of Biochar. *Fuel*, **2018**, *217*, 240–261. https://doi.org/https://doi.org/10.1016/j.fuel.2017.12.054.

[182] Chhimwal Monika and Pandey, D. and S. R. K. Pristine Biochar and Engineered Biochar: Differences and Application. In *Engineered Biochar: Fundamentals, Preparation, Characterization and Applications*; Ramola Sudipta and Mohan, D. and M. O. and M. A. and T. T., Ed.; Springer Nature Singapore: Singapore, 2022; pp 3–19. https://doi.org/10.1007/978-981-19-2488-0_1.

[183] Das, O.; Sarmah, A. K.; Bhattacharyya, D. Biocomposites from Waste Derived Biochars: Mechanical, Thermal, Chemical, and Morphological Properties. *Waste Management*, **2016**, *49*, 560–570. https://doi.org/https://doi.org/10.1016/j.wasman.2015.12.007.

[184] Ho, M.; Lau, K.; Wang, H.; Hui, D. Improvement on the Properties of Polylactic Acid (PLA) Using Bamboo Charcoal Particles. *Compos B Eng*, **2015**, *81*, 14–25. https://doi.org/https://doi.org/10.1016/j.compositesb.2015.05.048.

[185] You, H.; Hui, J.; Zhou, Y.; Vittore, K.; Zhang, J.; Chaney, L. E.; Chinta, S.; Zhao, Y.; Lim, G.; Lee, D.; et al. Sustainable Production of Biomass-Derived Graphite and Graphene Conductive Inks from Biochar. *Small*, **2024**, *20* (52). https://doi.org/10.1002/smll.202406669.

[186] Qian, K.; Kumar, A.; Zhang, H.; Bellmer, D.; Huhnke, R. Recent Advances in Utilization of Biochar. *Renewable and Sustainable Energy Reviews*, **2015**, *42*, 1055–1064. https://doi.org/https://doi.org/10.1016/j.rser.2014.10.074.

[187] Lehmann, J.; Cowie, A.; Masiello, C. A.; Kammann, C.; Woolf, D.; Amonette, J. E.; Cayuela, M. L.; Camps-Arbestain, M.; Whitman, T. Biochar in Climate Change Mitigation. *Nature Geoscience*. Nature Research December 1, 2021, pp 883–892. https://doi.org/10.1038/s41561-021-00852-8.

[188] Lee, J.; Kim, K. H.; Kwon, E. E. Biochar as a Catalyst. *Renewable and Sustainable Energy Reviews*. Elsevier Ltd 2017, pp 70–79. https://doi.org/10.1016/j.rser.2017.04.002.

[189] Huggins, T.; Wang, H.; Kearns, J.; Jenkins, P.; Ren, Z. J. Biochar as a Sustainable Electrode Material for Electricity Production in Microbial Fuel Cells. *Bioresour Technol*, **2014**, *157*, 114–119. https://doi.org/https://doi.org/10.1016/j.biortech.2014.01.058.

[190] Hu, Q.; Jung, J.; Chen, D.; Leong, K.; Song, S.; Li, F.; Mohan, B. C.; Yao, Z.; Prabhakar, A. K.; Lin, X. H.; et al. Biochar Industry to Circular Economy. *Science of The Total Environment*, **2021**, *757*, 143820. https://doi.org/https://doi.org/10.1016/j.scitotenv.2020.143820.

[191] Schmidt, H.; Kammann, C.; Hagemann, N.; Leifeld, J.; Bucheli, T. D.; Sánchez Monedero, M. A.; Cayuela, M. L. Biochar in Agriculture – A Systematic Review of 26 Global Meta-analyses. *Glob Change Biol Bioenergy*, **2021**, *13* (11), 1708–1730. https://doi.org/https://doi.org/10.1111/gcbb.12889.

[192] Giorcelli, M.; Khan, A.; Pugno, N. M.; Rosso, C.; Tagliaferro, A. Biochar as a Cheap and Environmental Friendly Filler Able to Improve Polymer Mechanical Properties. *Biomass Bioenergy*, **2019**, *120*, 219–223. https://doi.org/https://doi.org/10.1016/j.biombioe.2018.11.036.

[193] Vidakis, N.; Kalderis, D.; Petousis, M.; Maravelakis, E.; Mountakis, N.; Bolanakis, N.; Papadakis, V. Biochar Filler in MEX and VPP Additive Manufacturing: Characterization and Reinforcement Effects in Polylactic Acid and Standard Grade Resin Matrices. *Biochar*, **2023**, *5* (1). https://doi.org/10.1007/s42773-023-00238-6.

[194] Giorcelli, M.; Savi, P.; Khan, A.; Tagliaferro, A. Analysis of Biochar with Different Pyrolysis Temperatures Used as Filler in Epoxy Resin Composites. *Biomass Bioenergy*, **2019**, *122*, 466–471. https://doi.org/https://doi.org/10.1016/j.biombioe.2019.01.007.

[195] Senadheera, S. S.; Gupta, S.; Kua, H. W.; Hou, D.; Kim, S.; Tsang, D. C. W.; Ok, Y. S. Application of Biochar in Concrete – A Review. *Cem Concr Compos*, **2023**, *143*, 105204. https://doi.org/https://doi.org/10.1016/j.cemconcomp.2023.105204.

[196] Barbhuiya, S.; Bhusan Das, B.; Kanavaris, F. Biochar-Concrete: A Comprehensive Review of Properties, Production and Sustainability. *Case Studies in Construction Materials*, **2024**, *20*, e02859. https://doi.org/https://doi.org/10.1016/j.cscm.2024.e02859.

[197] Ferreira, G. F.; Pierozzi, M.; Fingolo, A. C.; da Silva, W. P.; Strauss, M. Tuning Sugarcane Bagasse Biochar into a Potential Carbon Black Substitute for Polyethylene Composites. *J Polym Environ*, **2019**, *27* (8), 1735–1745. https://doi.org/10.1007/s10924-019-01468-1.

[198] Peterson, S. C.; Chandrasekaran, S. R.; Sharma, B. K. Birchwood Biochar as Partial Carbon Black Replacement in Styrene–Butadiene Rubber Composites. *Journal of Elastomers & Plastics*, **2016**, *48* (4), 305–316. https://doi.org/10.1177/0095244315576241.

[199] Marchesini, J.; Perondi, D.; Marocco, M. V.; Pellizzoni, V. G.; Carberlon, G. O.; Godinho, M.; Piazza, D. Production and Application of Biochar in a UV Radiation-Curable Epoxy Paint as a Substitute for Graphite. *J Coat Technol Res*, **2023**, *20* (3), 957–971. https://doi.org/10.1007/s11998-022-00715-w.

[200] DebRoy T. and Bhadeshia, H. K. D. H. A Remarkable Innovation in Stainless Steel Making. In *Innovations in Everyday Engineering Materials*; Springer International Publishing: Cham, 2021; pp 1–7. https://doi.org/10.1007/978-3-030-57612-7_1.

[201] Ashby, M.; Shercliff, H.; Cebon, D. Chapter 2 - Family Trees: Organising Materials and Processes. In *Materials (Fourth Edition)*; Ashby, M., Shercliff, H., Cebon, D., Eds.; Butterworth-Heinemann, 2019; pp 15–30. https://doi.org/https://doi.org/10.1016/B978-0-08-102376-1.00002-0.

[202] Ashby, M.; Shercliff, H.; Cebon, D. Chapter 1 - Introduction: Materials – History and Character. In *Materials (Fourth Edition)*; Ashby, M., Shercliff, H., Cebon, D., Eds.; Butterworth-Heinemann, 2019; pp 1–14. https://doi.org/https://doi.org/10.1016/B978-0-08-102376-1.00001-9.

[203] Yusuf, M.; Shabbir, M.; Mohammad, F. Natural Colorants: Historical, Processing and Sustainable Prospects. *Natural Products and Bioprospecting*. Springer February 1, 2017, pp 123–145. https://doi.org/10.1007/s13659-017-0119-9.

[204] Alegbe, E. O.; Uthman, T. O. A Review of History, Properties, Classification, Applications and Challenges of Natural and Synthetic Dyes. *Heliyon*, **2024**, *10* (13), e33646. https://doi.org/https://doi.org/10.1016/j.heliyon.2024.e33646.

[205] Bechtold, T.; Pham, T. Natural Colorants in the Mass Coloration of Plastics. In *Handbook of Natural Colorants*; John Wiley & Sons, Ltd, 2023; pp 557–562. https://doi.org/https://doi.org/10.1002/9781119811749.ch26.

[206] Goktas, O.; Ozen, E.; Baysal, E.; Mammadov, R.; Alma, M. H.; Sonmez, A. Color Stability of Wood Treated with Madder Root (Rubia Tinctorium) Extract after Lightfastness Test. *Wood Research*, **2009**, *54* (1), 37–44.

[207] Virgili, T.; Pasini, M.; Guizzardi, M.; Tizro, N.; Bollani, M. Natural Dyes Used as Organic Coatings UV Protecting for Food Packages. *Coatings*, **2022**, *12* (3). https://doi.org/10.3390/coatings12030417.

[208] Weigl-Kuska, M.; Kandelbauer, A.; Hansmann, C.; Müller, U. Wood—From Natural Color Patterns Toward Naturally Altered Color Impressions. In *Handbook of Natural Colorants*; John Wiley & Sons, Ltd, 2023; pp 469–505. https://doi.org/https://doi.org/10.1002/9781119811749.ch22.

[209] Bulian, F.; Graystone, J. A. Chapter 7 - Market Needs and End Uses (1) – Architectural (Decorative) Wood Coatings. In *Wood Coatings*; Bulian, F., Graystone, J. A., Eds.; Elsevier: Amsterdam, 2009; pp 195–231. https://doi.org/https://doi.org/10.1016/B978-0-444-52840-7.00007-2.

[210] Bulian, F.; Graystone, J. A. Chapter 8 - Market Needs and End Uses (2) – Industrial Wood Coatings. In *Wood Coatings*; Bulian, F., Graystone, J. A., Eds.; Elsevier: Amsterdam, 2009; pp 233–258. https://doi.org/https://doi.org/10.1016/B978-0-444-52840-7.00008-4.

[211] Sakhno, T. V.; Barashkov, N. N.; Irgibaeva, I. S.; Pustovit, S. V.; Sakhno, Y. E. Polymer Coatings for Protection of Wood and Wood-Based Materials. *Advances in Chemical Engineering and Science*, **2016**, *06* (02), 93–110. https://doi.org/10.4236/aces.2016.62012.

[212] Landry, V.; Boivin, G.; Schorr, D.; Mottoul, M.; Mary, A.; Abid, L.; Carrère, M.; Laratte, B. Recent Developments and Trends in Sustainable and Functional Wood Coatings. *Current Forestry Reports*. Springer Science and Business Media Deutschland GmbH October 1, 2023, pp 319–331. https://doi.org/10.1007/s40725-023-00195-0.

[213] Nejad, M.; Cooper, P. Exterior Wood Coatings. In *Wood in Civil Engineering*; Concu, G., Ed.; IntechOpen: Rijeka, 2017. https://doi.org/10.5772/67170.

[214] Reinprecht, L.; Pánek, M. Effects of Wood Roughness, Light Pigments, and Water Repellent on the Color Stability of Painted Spruce Subjected to Natural and Accelerated Weathering. *Bioresources*, **2015**, *10* (4), 7203–7219. https://doi.org/10.15376/biores.10.4.7203-7219.

[215] Peng, Y.; Wang, Y.; Chen, P.; Wang, W.; Cao, J. Enhancing Weathering Resistance of Wood by Using Bark Extractives as Natural Photostabilizers in Polyurethane-Acrylate Coating. *Prog Org Coat*, **2020**, *145*. https://doi.org/10.1016/j.porgcoat.2020.105665.

[216] Özgenç, Ö.; Bilici, E.; Durmaz, S.; Söğütlü, C.; Emik, S. Enhancing Weathering Durability of Pre-Protected and Unprotected Wood by Using Bark Extracts as Natural UV Absorbers in Waterborne Acrylic Coating. *J Coat Technol Res*, **2022**, *19* (1), 303–321. https://doi.org/10.1007/s11998-021-00528-3.

[217] Etzrodt, G. 4 - Basics of Colorants. In *Industrial Coloration of Plastics*; Etzrodt, G., Ed.; Hanser, 2021; pp 27–32. https://doi.org/https://doi.org/10.3139/9781569908532.004.

[218] Etzrodt, G. 5 - Colorant Properties and Test Methods. In *Industrial Coloration of Plastics*; Etzrodt, G., Ed.; Hanser, 2021; pp 33–57. https://doi.org/https://doi.org/10.3139/9781569908532.005.

[219] Charvat, R. A. Introduction to Colorants. In *Coloring of Plastics*; John Wiley & Sons, Ltd, 2003; pp 85–99. https://doi.org/https://doi.org/10.1002/0471721581.ch7.

[220] García, A. M.; García, A. I.; Cabezas, M. Á. L.; Reche, A. S. Study of the Influence of the Almond Variety in the Properties of Injected Parts with Biodegradable Almond Shell Based Masterbatches. *Waste Biomass Valorization*, **2015**, *6* (3), 363–370. https://doi.org/10.1007/s12649-015-9351-x.

[221] Suaduang, N.; Ross, S.; Ross, G. M.; Pratumshat, S.; Mahasaranon, S. Effect of Spent Coffee Grounds Filler on the Physical and Mechanical Properties of Poly(Lactic Acid) Bio-Composite Films. *Mater Today Proc*, **2019**, *17*, 2104–2110. https://doi.org/https://doi.org/10.1016/j.matpr.2019.06.260.

[222] Velho, S. R. K.; Brum, L. F. W.; Petter, C. O.; dos Santos, J. H. Z.; Šimunić, Š.; Kappa, W. H. Development of Structured Natural Dyes for Use into Plastics. *Dyes and Pigments*, **2017**, *136*, 248–254. https://doi.org/https://doi.org/10.1016/j.dyepig.2016.08.021.

[223] Latos, M.; Masek, A.; Zaborski, M. The Potential of Juglone as Natural Dye and Indicator for Biodegradable Polyesters. *Proceedings of the Institution of Mechanical Engineers, Part L: Journal of Materials: Design and Applications*, **2019**, *233* (3), 276–285. https://doi.org/10.1177/1464420718804271.

[224] Abidin, Z. H. Z.; Naziron, N. N.; Nasir, K. M.; Rusli, M. S.; Lee, S. V; Kufian, M. Z.; Majid, S. R.; Vengadaesvaran, B.; Arof, A. K.; Taha, R. M.; et al. Influence of Curcumin Natural Dye Colorant with PMMA-acrylic Polyol Blended Polymer. *Pigment & Resin Technology*, **2013**, *42* (2), 95–102. https://doi.org/10.1108/03699421311301070.

[225] Van Den Oever, M. J. A.; Boeriu, C. G.; Blaauw, R.; Van Haveren, J. Colorants Based on Renewable Resources and Food-Grade Colorants for Application in Thermoplastics. *J Appl Polym Sci*, **2004**, *92* (5), 2961–2969. https://doi.org/https://doi.org/10.1002/app.20298.

[226] Pedeferri, P. Corrosion Prevention by Coatings. In *Engineering Materials*; Springer Science and Business Media B.V., 2018; pp 327–361. https://doi.org/10.1007/978-3-319-97625-9_17.

[227] Dong, L.; Li, Y.; Huang, M.; Hu, X.; Qu, Z.; Lu, Y. Effect of Anodizing Surface Morphology on the Adhesion Performance of 6061 Aluminum Alloy. *Int J Adhes Adhes*, **2022**, *113*, 103065. https://doi.org/https://doi.org/10.1016/j.ijadhadh.2021.103065.

[228] Bargui, M.; Elleuch, K.; Wery, M.; Ayedi, H. F. Optimization of Mechanical and Tribological Properties of Anodized 5754 Aluminium Alloy. *Surface Engineering and Applied Electrochemistry*, **2017**, *53* (4), 371–382. https://doi.org/10.3103/S1068375517040020.

[229] Ali, I.; Quazi, M. M.; Zalnezhad, E.; Sarhan, A. A. D.; Sukiman, N. L.; Ishak, M. Hard Anodizing of Aerospace AA7075-T6 Aluminum Alloy for Improving Surface Properties. *Transactions of the Indian Institute of Metals*, **2019**, *72* (10), 2773–2781. https://doi.org/10.1007/s12666-019-01754-5.

[230] Elkilany, H. A.; Shoeib, M. A.; Abdel-Salam, O. E. Influence of Hard Anodizing on the Mechanical and Corrosion Properties of Different Aluminum Alloys. *Metallography,*

Microstructure, and Analysis, **2019**, *8* (6), 861–870. https://doi.org/10.1007/s13632-019-00594-5.

[231] Tsangaraki-Kaplanoglou, I.; Moshohoritou, R.; Kallithrakas-Kontos, N. The Use of a Natural Dye in the Formation of a Thin Coloured Coating on an Aluminium Surface. *Journal of the Society of Dyers and Colourists*, **1989**, *105* (3), 114–119. https://doi.org/https://doi.org/10.1111/j.1478-4408.1989.tb01201.x.

[232] Setyawan, P. E.; Sonalitha, E.; Asmono, D. A.; Refitra, R. A. Investigation of the Effect of Anodizing Dyes Using Purple Cabbage and Dragon Fruit Peel on Aluminum 6061alloy. *International Journal of Advances in Scientific Research and Engineering*, **2021**, *07* (02), 15–27. https://doi.org/10.31695/ijasre.2021.33971.

[233] Farid, A.; Wibowo, H.; MK, I. Analysis Of Thickness And Brightness Of Aluminum Layers In The Anodizing Process With Various Types Of Coloring And Process Times. *Mestro: Jurnal Teknik Mesin dan Elektro*, **2024**, *6* (02), 1–5. https://doi.org/10.47685/mestro.v6i02.565.

[234] Tonapa Sarungu, Y. Pemanfaatan Ekstrah Kulit Buah Manggis Sebagai Pewarna Logam Aluminium. In *Industrial Research Workshop and National Seminar*; 2012; Vol. 3. https://doi.org/10.35313/irwns.v3i0.428.

[235] Muslim, A.; Widyo Nugroho, A. Karakterisasi Permukaan Pada Aluminium Anodized-Dyed Dengan Pewarna Alami Kunyit. *JMPM (Jurnal Material dan Proses Manufaktur)*, **2018**, *2* (1). https://doi.org/10.18196/jmpm.2117.

[236] J. Juita; Dlugogorski, B. Z.; Kennedy, E. M.; Mackie, J. C. Low Temperature Oxidation of Linseed Oil: A Review. *Fire Sci Rev*, **2012**, *1* (1), 3. https://doi.org/10.1186/2193-0414-1-3.

[237] Derksen, J. T. P.; Cuperus, F. P.; Kolster, P. Renewable Resources in Coatings Technology: A Review. *Prog Org Coat*, **1996**, *27* (1–4), 45–53. https://doi.org/10.1016/0300-9440(95)00518-8.

[238] Green, A. G.; Marshall, D. R. Variation for Oil Quantity and Quality in Linseed (Linum Usitatissimum). *Aust. J. Agric. Res*, **1981**, *32*, 599–607.

[239] Baran, A.; Fiedler, A.; Schulz, H.; Baranska, M. In Situ Raman and IR Spectroscopic Analysis of Indigo Dye. *Analytical Methods*, **2010**, *2* (9), 1372–1376. https://doi.org/10.1039/c0ay00311e.

[240] Mahltig, B. Overview on Natural Dyes and Their IR-Spectra – Part II: Indigo Containing Plant Dyes. *Communications in Development and Assembling of Textile Products*, **2024**, *5* (1), 66–80. https://doi.org/10.25367/cdatp.2024.5.p66-80.

[241] Sousa, M.; Miguel, C.; Rodrigues, I.; Parola, A. J.; Pina, F.; Melo, J. S.; Melo, M. A Photochemical Study on the Blue Dye Indigo: From Solution to Ancient Andean Textiles. *Photochem Photobiol Sci*, **2008**, *7*, 1353–1359. https://doi.org/10.1039/b809578g.

[242] Vautier, M.; Guillard, C.; Herrmann, J.-M. Photocatalytic Degradation of Dyes in Water: Case Study of Indigo and of Indigo Carmine. *J Catal*, **2001**, *201* (1), 46–59. https://doi.org/https://doi.org/10.1006/jcat.2001.3232.

[243] Lazzari, M.; Chiantore, O. Drying and Oxidative Degradation of Linseed Oil. *Polym Degrad Stab*, **1999**, *65* (2), 303–313. https://doi.org/10.1016/S0141-3910(99)00020-8.

[244] Orlova, Y.; Harmon, R. E.; Broadbelt, L. J.; Iedema, P. D. Review of the Kinetics and Simulations of Linseed Oil Autoxidation. *Progress in Organic Coatings*. Elsevier B.V. February 1, 2021. https://doi.org/10.1016/j.porgcoat.2020.106041.

[245] Goutam, S. P.; Saxena, G.; Singh, V.; Yadav, A. K.; Bharagava, R. N.; Thapa, K. B. Green Synthesis of TiO2 Nanoparticles Using Leaf Extract of Jatropha Curcas L. for Photocatalytic Degradation of Tannery Wastewater. *Chemical Engineering Journal*, **2018**, *336*, 386–396. https://doi.org/10.1016/j.cej.2017.12.029.

[246] Meilunas, R. J.; Bentsen, J. G.; Steinberg, A.; Steinb, A. Analysis of Aged Paint Binders by FTIR Spectroscopy. *Studies in Conservation*, **1990**, *35* (1), 33–51. https://doi.org/10.2307/1506280.

[247] Schmitt, T.; Rosi, F.; Mosconi, E.; Shull, K.; Fantacci, S.; Miliani, C.; Gray, K. New Insights into the Deterioration of TiO2 Based Oil Paints: The Effects of Illumination Conditions and Surface Interactions. *Herit Sci*, **2022**, *10* (1). https://doi.org/10.1186/s40494-022-00733-2.

[248] Maier, C.; Calafut, T. Design Principles. In *Polypropylene*; Maier, C., Calafut, T., Eds.; Plastics Design Library; William Andrew Publishing: Norwich, NY, 1998; pp 109–144. https://doi.org/https://doi.org/10.1016/B978-188420758-7.50017-5.

[249] Fang, J.; Zhang, L.; Sutton, D.; Wang, X.; Lin, T. Needleless Melt-Electrospinning of Polypropylene Nanofibres. *J Nanomater*, **2012**, *2012*. https://doi.org/10.1155/2012/382639.

[250] Mylläri, V.; Ruoko, T. P.; Syrjälä, S. A Comparison of Rheology and FTIR in the Study of Polypropylene and Polystyrene Photodegradation. *J Appl Polym Sci*, **2015**, *132* (28). https://doi.org/10.1002/app.42246.

[251] Uheida, A.; Mejía, H. G.; Abdel-Rehim, M.; Hamd, W.; Dutta, J. Visible Light Photocatalytic Degradation of Polypropylene Microplastics in a Continuous Water Flow System. *J Hazard Mater*, **2021**, *406*, 124299. https://doi.org/https://doi.org/10.1016/j.jhazmat.2020.124299.

[252] Nichols, J. A.; Katiyar, S. K. Skin Photoprotection by Natural Polyphenols: Anti-Inflammatory, Antioxidant and DNA Repair Mechanisms. *Archives of Dermatological Research*. 2010, pp 71–83. https://doi.org/10.1007/s00403-009-1001-3.

[253] Chowdhury, P.; Nag, S.; Ray, A. K. Degradation of Phenolic Compounds Through UV and Visible- Light-Driven Photocatalysis: Technical and Economic Aspects. In *Phenolic Compounds - Natural Sources, Importance and Applications*; InTech, 2017. https://doi.org/10.5772/66134.

[254] Kim, Y.; Suhr, J.; Seo, H. W.; Sun, H.; Kim, S.; Park, I. K.; Kim, S. H.; Lee, Y.; Kim, K. J.; Nam, J. Do. All Biomass and UV Protective Composite Composed of Compatibilized Lignin and Poly (Lactic-Acid). *Sci Rep*, **2017**, *7* (1). https://doi.org/10.1038/srep43596.

[255] Wu, X.; Lian, H.; Xia, C.; Deng, J.; Li, X.; Zhang, C. Mechanistic Insights and Applications of Lignin-Based Ultraviolet Shielding Composites: A Comprehensive Review. *International Journal of Biological Macromolecules*. Elsevier B.V. November 1, 2024. https://doi.org/10.1016/j.ijbiomac.2024.135477.

[256] Choinska, E.; Muroya, T.; Swieszkowski, W.; Aoyagi, T. Influence of Macromolecular Structure of Novel 2- and 4-Armed Polylactides on Their Physicochemical Properties and in Vitro Degradation Process. *Journal of Polymer Research*, **2016**, *23* (7). https://doi.org/10.1007/s10965-016-1023-4.

[257] Sato, S.; Ono, M.; Yamauchi, J.; Kanehashi, S.; Ito, H.; Matsumoto, S.; Iwai, Y.; Matsumoto, H.; Nagai, K. Effects of Irradiation with Vacuum Ultraviolet Xenon Excimer Lamp at 172nm on Water Vapor Transport through Poly(Lactic Acid) Membranes. *Desalination*, **2012**, *287*, 290–300. https://doi.org/10.1016/j.desal.2011.08.026.

[258] Vasanthan, N.; Ly, O. Effect of Microstructure on Hydrolytic Degradation Studies of Poly (l-Lactic Acid) by FTIR Spectroscopy and Differential Scanning Calorimetry. *Polym Degrad Stab*, **2009**, *94* (9), 1364–1372. https://doi.org/10.1016/j.polymdegradstab.2009.05.015.

[259] Ikada, E. Photo-and Bio-Degradable Polyesters. Photodegradation Behaviors of Aliphatic Polyesters. *Journal of Photopolymer Science and Technology*, **1997**, *10* (2), 265–270. https://doi.org/10.2494/photopolymer.10.265.

[260] Izadi-Vasafi, H.; Mohamad Sadeghi, G. M.; Garmabi, H. Synthesis of Hydroxyl-Terminated Poly(Lactic Acid) via Polycondensation: An Equation to Predict Molecular Weight Based on the Reaction Parameters. *J Appl Polym Sci*, **2012**, *125* (SUPPL. 2). https://doi.org/10.1002/app.36636.

[261] Hablot, E.; Dharmalingam, S.; Hayes, D. G.; Wadsworth, L. C.; Blazy, C.; Narayan, R. Effect of Simulated Weathering on Physicochemical Properties and Inherent Biodegradation of

PLA/PHA Nonwoven Mulches. *J Polym Environ*, **2014**, *22* (4), 417–429. https://doi.org/10.1007/s10924-014-0697-0.

[262] Janorkar, A. V.; Metters, A. T.; Hirt, D. E. Degradation of Poly(L-Lactide) Films under Ultraviolet-Induced Photografting and Sterilization Conditions. *J Appl Polym Sci*, **2007**, *106* (2), 1042–1047. https://doi.org/10.1002/app.24692.

[263] Zaidi, L.; Kaci, M.; Bruzaud, S.; Bourmaud, A.; Grohens, Y. Effect of Natural Weather on the Structure and Properties of Polylactide/Cloisite 30B Nanocomposites. *Polym Degrad Stab*, **2010**, *95* (9), 1751–1758. https://doi.org/10.1016/j.polymdegradstab.2010.05.014.

[264] González-López, M. E.; Martín del Campo, A. S.; Robledo-Ortíz, J. R.; Arellano, M.; Pérez-Fonseca, A. A. Accelerated Weathering of Poly(Lactic Acid) and Its Biocomposites: A Review. *Polymer Degradation and Stability*. Elsevier Ltd September 1, 2020. https://doi.org/10.1016/j.polymdegradstab.2020.109290.

[265] Lizárraga-Laborín, L. L.; Quiroz-Castillo, J. M.; Encinas-Encinas, J. C.; Castillo-Ortega, M. M.; Burruel-Ibarra, S. E.; Romero-García, J.; Torres-Ochoa, J. A.; Cabrera-Germán, D.; Rodríguez-Félix, D. E. Accelerated Weathering Study of Extruded Polyethylene/Poly (Lactic Acid)/Chitosan Films. *Polym Degrad Stab*, **2018**, *155*, 43–51. https://doi.org/10.1016/j.polymdegradstab.2018.06.007.

[266] Martín del Campo, A. S.; Robledo-Ortíz, J. R.; Arellano, M.; Rabelero, M.; Pérez-Fonseca, A. A. Accelerated Weathering of Polylactic Acid/Agave Fiber Biocomposites and the Effect of Fiber–Matrix Adhesion. *J Polym Environ*, **2021**, *29* (3), 937–947. https://doi.org/10.1007/s10924-020-01936-z.

[267] Ito, M.; Abe, S.; Ishikawa, M. The Fracture Mechanism of Polylactic Acid Resin and the Improving Mechanism of Its Toughness by Addition of Acrylic Modifier. *J Appl Polym Sci*, **2010**, *115* (3), 1454–1460. https://doi.org/https://doi.org/10.1002/app.31292.

[268] Ye, H.; You, T.; Nawaz, H.; Xu, F. A Comprehensive Review on Polylactic Acid/Lignin Composites — Structure, Synthesis, Performance, Compatibilization, and Applications. *International Journal of Biological Macromolecules*. Elsevier B.V. November 1, 2024. https://doi.org/10.1016/j.ijbiomac.2024.135886.

[269] Stevenson, M. F. Anodizing. In *Surface Engineering*; ASM International, 1994; pp 482–493. https://doi.org/10.31399/asm.hb.v05.a0001281.

[270] Knutsson, L.; Dahlberg, K. Lightfastness and Corrosion Resistance of Colour Anodized Aluminium. *Transactions of the IMF*, **1976**, *54* (1), 53–55. https://doi.org/10.1080/00202967.1976.11870373.

[271] Patel, P.; Patel, T. Coloring Anodized Aluminum. In *Aluminum Science and Technology*; ASM International, 2018; pp 611–615. https://doi.org/10.31399/asm.hb.v02a.a0006512.

Appendix 1: Key terms of the research

English:

Key term: biocolorant
Definition: organic dye or pigment extracted from natural origin
Explanation: Biocolorants are organic dyes or pigments extracted from natural origins, such as plants, fungi, or algae.

Key term: engineering material
Definition: human-manufactured solid material, which is frequently used in structural and/or mechanical applications
Explanation: Engineering material is a phrase commonly used to describe a large group of human-manufactured solid materials, which are frequently used in structural and/or mechanical applications. Engineering materials include, for instance, metals, plastics, ceramics, and composites.

Finnish:

Keskeinen termi: luonnonväri
Määritelmä: orgaaninen luonnosta peräisin oleva väriaine
Selite: Luonnonvärit ovat orgaanisia väriaineita, jotka ovat peräisin luonnosta. Luonnonvärejä ovat esimerkiksi, kasvien, sienten, tai levien aineenvaihdunnan tuotoksena syntyvät väriaineet.

Keskeinen termi: tekninen materiaali
Määritelmä: ihmisen valmistama tai olennaisesti muokkaama kiinteä materiaali, jota käytetään yleisesti rakenteellisissa tai mekaanisissa sovelluskohteissa
Selite: Tekninen materiaali on kattokäsite suurelle joukolle ihmisen valmistamia kiinteitä materiaaleja, joita käytetään rakenteellisissa tai mekaanisissa sovellutuksissa. Teknisiä materiaaleja ovat muun muassa metallit, muovit, keraamit sekä komposiitit.

Business, Economy
Art, Design, Architecture
Science, Technology
Crossover
Doctoral Theses

Aalto DT 198/2025

ISBN 978-952-64-2767-6
ISBN 978-952-64-2766-9 (pdf)

Aalto University
School of Chemical Engineering
Department of Chemistry and
Materials Science
aalto.fi